JOURNAL OF GEOPHYSICAL RESEARCH, VOL. 104, NO. A12, PAGES 28,565–28,586, DECEMBER 1, 1999

Sporadic plasma sheet ion injections into the high-altitude auroral bulge: Satellite observations

J.-A. Sauvaud,[1] D. Popescu,[1] D. C. Delcourt,[2] G. K. Parks,[3] M. Brittnacher,[3] V. Sergeev,[4] R. A. Kovrazhkin,[5] T. Mukai,[6] and S. Kokubun[7]

Abstract. We report on a new feature of auroral substorms, namely, the sporadic though recurrent injections of magnetospheric ions throughout the auroral bulge. These injections are interpreted as time of flight dispersed ion structures (TDIS). Our analysis builds on a combination of measurements from Interball-Auroral, from UV imagery onboard Polar, from ground magnetometers, and also from observations on Geotail and from geostationary spacecraft. Backward tracing of ion trajectories from Interball-Auroral orbit using realistic three-dimensional magnetic and electric field models indicates that the injection region can extend over a wide range of radial distances, from ~7–40 R_E in the nearly equatorial magnetosphere. Both hydrogen and oxygen ions are shown to be injected toward the Earth's upper ionosphere. At Interball altitudes we find that ion injections are associated with two types of low-frequency torsional oscillations of the magnetic field: (1) shear Alfvén waves with a period of a few minutes with the highest amplitude near the bulge front and decreasing amplitude at lower latitudes and (2) higher-frequency shear Alfvén waves of the P1B type, strictly restricted to the poleward boundary of the surge, with a characteristic period of ~40 s. The systematic observation of sporadic TDIS during the auroral bulge expansion leads us to conclude that the same physical process is at work throughout the midtail. We also show that ion injections are detected well inside the bulge, which suggests that the injection fronts propagate from the outer to the inner magnetosphere over large distances. This topic is more extensively studied by *Sergeev et al.* [1999]. We also show that the poleward boundary of the surge is associated with a prominent outflow of ionospheric H^+ and O^+. These ions in the hundred of eV to the keV range are heated perpendicularly to the local magnetic field and subsequently transported into the magnetotail. The expanding auroral bulge thus forms a significant source of ionospheric ions for the midtail magnetosphere.

1. Introduction

Assessing the large-scale dynamics of the magnetospheric system during substorms has motivated a number of studies in the recent years, and it is still one of the main areas of magnetospheric research. Magnetic field observations in the equatorial region of the inner magnetosphere and farther in the magnetotail lobe have shown that a reconfiguration of the magnetic field topology ("dipolarization") linked to a partial disruption of the near-Earth cross-tail current is associated with substorm onsets detected as breakups of auroral forms in the ionosphere [e.g., *Sauvaud and Winckler*, 1980; *Lui*, 1988, 1996; *Lopez and Lui*, 1990; *Jacquey et al*., 1991, 1993; *Ohtani et al*., 1992]. Many plasma processes linked to substorms have been identified in the tail, such as the formation of a thin current sheet before substorm onset, and earthward plasma injections within the inner magnetosphere associated with impulsive plasma sheet thinnings at onset [e.g., *Winckler*, 1969, *Sauvaud et al*., 1984; *Pulkkinen et al*., 1994]. The location and shape of the inner boundary of particle injections associated with substorms have been established from observations of energetic charged particles at geosynchronous orbit [e.g., *McIlwain*, 1974; *Mauk and McIlwain*, 1974; *Quinn and McIlwain*, 1979]. The acceleration mechanism producing the injection boundary has been investigated in detail by a number of theoretical and numerical studies [*Quinn and Southwood*, 1982; *Mauk*, 1986; *Delcourt et al*., 1990; *Lewis et al*., 1990; *Delcourt and Sauvaud*, 1994; *Delcourt et al*., 1997]. All are based on the "convection surge" process, which invokes a strong though temporary increase of the electric field as suggested by in situ measurements [*Aggson et al*., 1983]. Farther in the plasma sheet, at distances of the order of 18 R_E, statistical studies show that the plasma sheet thins almost simultaneously with particle injections at 6.6 R_E [e.g., *Sauvaud et al*., 1984]. According to *Kan* [1998], the time delay between dipolarization and thinning is equal to or greater than the fast-mode propagation time from the dipolarization region, i.e., ~1 min per R_E.

In the distant tail the ejection in the antisolar direction of energetic electrons and ions closely follows the appearance of magnetic bays in the auroral zone [e.g., *Bieber et al*., 1980; *Scholer et al*., 1986; *Jacquey et al*., 1994]. Later during substorm events, other typical processes have been recorded in situ, such

[1]Centre d'Etude Spatiale des Rayonnements, Toulouse, France.
[2]Centre d'Etude des Environnement Terrestres et Planétaires, Saint-Maur des Fossés, France.
[3]Geophysics Department, University of Washington, Seattle.
[4]University of St. Petersburg, St. Petersburg, Russia.
[5]Institute of Space Research, IKI, Moscow, Russia.
[6]Institute of Space and Astronautical Science, Tokyo, Japan.
[7]Solar Terrestrial Environmental Laboratory, Nagoya University, Nagoya, Japan.

Paper number 1999JA900293.
0148-0227/99/1999JA900293$09.00

as the plasma sheet recovery (thickening) and the release of plasmoids from the far tail [e.g., *Hones et al*., 1967, 1984; *Scholer et al*., 1984; *Sauvaud et al*., 1996; *Nagai et al*., 1997, 1998].

All the processes discussed so far are generally presented as single entities; i.e., an isolated substorm would be associated with a single injection, a plasma sheet thinning, and a plasmoid formation. There are, however, numerous experimental pieces of evidence showing that even single substorms are made of recurrent and impulsive processes. The most striking experimental evidences have been presented from ground measurements by *Sergeev and Yahnin* [1979], *Tighe and Rostoker* [1981], *Rostoker et al*. [1987], and *Bösinger and Yahnin* [1987], who showed that the auroral surge phenomenon did not consist of a single form propagating westward and poleward. Rather, it is characterized by a progressive reappearance of localized, short-lived (a few minutes) activations, each new arc system appearing to the north of the preceding one. This bears a close resemblance with a recent work by *Angelopoulos et al*. [1996], who found from correlated satellite and ground data that during the course of a substorm expansion phase the tailward progression of acceleration center in the tail is really the reappearance of new acceleration regions at gradually more tailward sites. *Sergeev et al*. [1992, 1996] also argued that impulsive dissipation events observed in energetic particles, electric fields, and plasma data in the magnetotail exhibit, during fortuitous conjunctions with the ground, a good one to one correlation with ionospheric activity intensifications. Such intensifications are often composed of a sequence of appearance of localized, short-lived (a few minutes) activations at progressively higher latitudes.

The orbit of Interball-Auroral, which slowly (~1 km/s) skims through the midnight sector at altitudes of the order of 3 R_E, provides a unique opportunity to study remotely the magnetotail activations when auroral bulges engulf the satellite. The spacecraft altitude is such that near apogee Interball-Auroral sits above the main auroral acceleration region and is able to detect the signatures of processes acting in the tail during substorms. In the present paper we report on sporadic, recurrent ion injections linked both to the northward boundary of the auroral bulge and to more southward regions of the bulge. Our goal is twofold: (1) to study the location, recurrence, and main characteristics of the ion injections and to give a preliminary description of the associated low-frequency waves and (2) to deduce from the data some constraints on the source extension in the equatorial magnetosphere. Our analysis is based on a combination of Interball plasma and magnetic field data, Polar UV measurements, and data taken simultaneously on the ground, at 6.6 R_E onboard the LANL spacecraft, and inside the tail onboard Geotail. A paper by *Sergeev et al*. [1999] is devoted to detailed comparisons between successive ion injections and small-scale auroral activations measured from all-sky cameras and magnetometers.

In particular, we will show that during substorm expansion phase two main ion injection types (H^+) are observed: (1) as initially reported by *Quinn and McIlwain* [1979], bouncing ion clusters injected from the equatorial inner magnetosphere and, (2) sporadic injections with no detectable bounces in the poleward part of the auroral bulge. These latter injections are shown to originate from a time-varying source in the midtail and to follow from time of flight effects (hence their denomination as time of flight dispersed ion structures (TDIS)). In several cases, O^+ injections are also observed. These observations lead us to conclude that during the expansion phase of substorms, a general physical process is sporadically acting in the outer magnetosphere from ~8 to 40 R_E, progressing northward (tailward) with the bulge and featuring a characteristic timescale in the minute range.

2. Data Sources

We investigated discrete ion signatures in the nightside auroral oval during substorms using the ION experiment flown on the Russian Interball-Auroral satellite (Interball-2), simply referred as Interball hereinafter. This spacecraft was launched on August 29, 1996, into a 62.8° inclination orbit with an apogee altitude of ~3 R_E. The satellite orbital period is ~6 hours. It is slowly spinning, at a rate of 0.5 rpm. The satellite was still operating in the winter of 1998–1999. All events presented in this paper are taken near the satellite apogee, in the midnight sector.

The ION experiment was developed to measure both auroral ions and electrons. This experiment comprises two mass spectrometers (Wien filters) and two simple electron detectors [*Sauvaud et al*., 1998]. The mass spectrometers are looking in opposite directions, perpendicularly to the satellite spin axis, which points toward the Sun. They measure H^+ and O^+ ions in the energy range ~0–14,000 eV/q. The two electron spectrometers are also looking in opposite directions and perform measurements in the energy range ~10 to 20,000 eV. The time required to sample a full energy spectrum varies from 1.5 to 6 s depending of the operation mode. The magnetic field vector is given by a fluxgate sensor with a time resolution which can be varied between 1/16 and 3 s, this latter resolution being used throughout this paper.

The measurements made with Interball are correlated with far UV images from Polar. The instrument is designed to operate over a wavelength range from 1300 to 1900 Å, i.e., to measure the Lyman-Birge-Hopfield system of bands, which results from electron impact ionization of N_2. LBH bands are detected in two segments, one at short wavelength (LBHS) where strong absorption in the Shuman Runge continuum occurs, and one at longer wavelengths (LBHL) where the O_2 absorption is not significant [*Torr et al*., 1995].

Both the UV images from Polar and the magnetic field data from the 210MM and IMAGE magnetometer chains are used to characterize the magnetospheric conditions and identify substorm phases. The time resolution of the magnetic field data from IMAGE and the 210MM chains are respectively 10 s and 1 min. The geosynchronous satellite LANL 1994-084 also provided ion and electron fluxes in the energy range from 50 to 1500 keV, with a time resolution of 1 min. Finally, Interball data were correlated with plasma and magnetic field measurements from the LEP-EA and MGF instruments installed onboard Geotail. Detailed descriptions of these instruments are given by *Mukai et al*. [1994] and *Kokubun et al*. [1995] respectively. In the present analysis, we use data averaged over every four spins (~12 s) for LEP-EA and spin-averaged data for MGF.

3. Observations

3.1. H^+ Multiple Bouncing Ion Clusters Associated With Auroral Bulge

The first example of dispersed ion structures we will examine pertains to a period of overall very quiet magnetic activity on

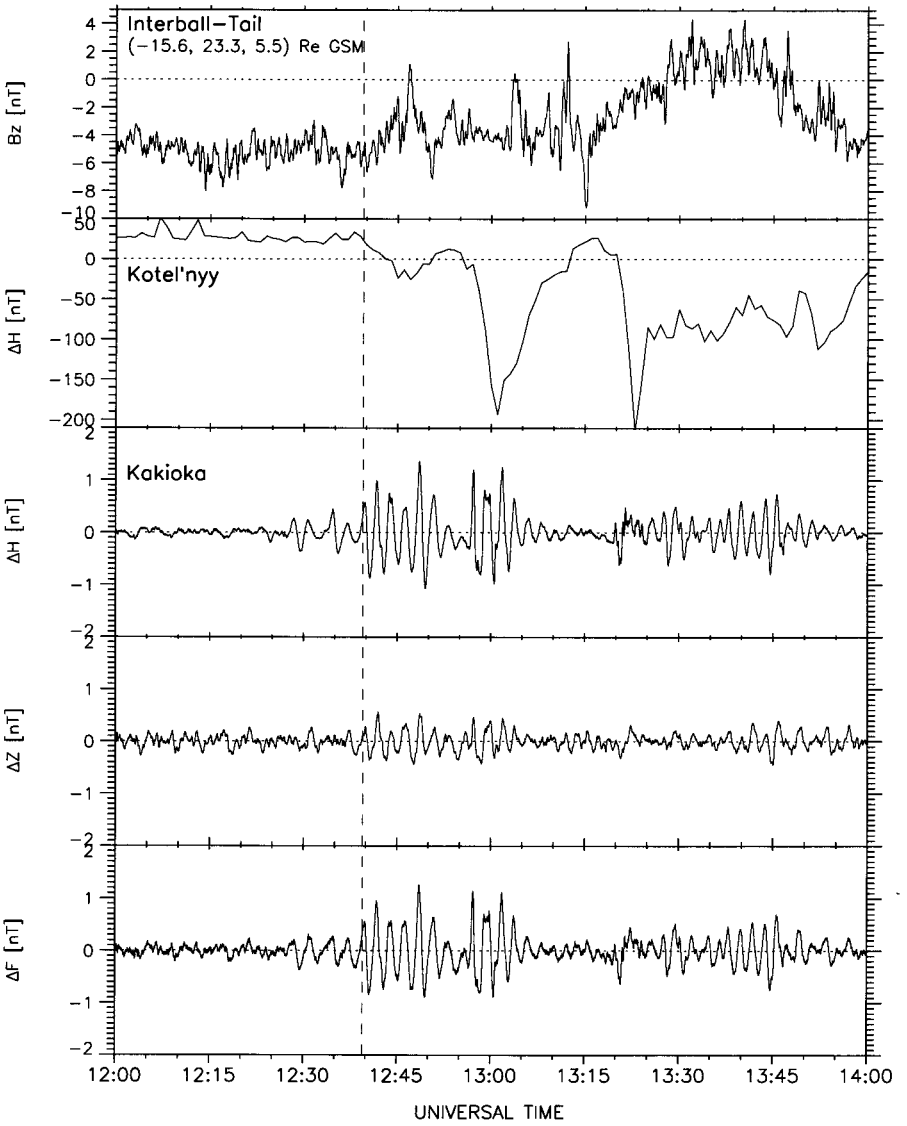

Figure 1. Interplanetary and ground measurements on January 17, 1997. (top to bottom) The northward component of the interplanetary magnetic field measured onboard Interball-Tail in the solar wind. The horizontal component of the geomagnetic field measured at Kotel'nyy (210MM chain) at an invariant latitude of 69.94° and a magnetic local time of UT + 8.4 hours. The filtered components of the geomagnetic field at the Kakioka midlatitude station (MLT = UT + 9.2 hours). The vertical dashed line marks the substorm onset at ~1239 UT.

January 17, 1997 ($Kp = 0_0$). An auroral breakup occurs at ~1239 UT as identified by Pi2 pulsations at Kakioka (MLT = 21.85 H). The substorm takes place during a period of southward directed IMF as deduced from the magnetic field data from Interball-Tail (Figure 1). This latter spacecraft was located at $X_{GSM} = -15.6$, $Y_{GSM} = 23.3$, and $Z_{GSM} = 5.5\ R_E$, in the solar wind according to in situ plasma measurements. In Figure 1, the horizontal component of the magnetic field at Kotel'nyy station (INVLAT = 69.94°) from the 210MM Magnetic Meridian chain is also shown. Kotel'nyy displays a weak negative bay starting around 1239–1240 UT. At that time, Interball crossed the auroral oval in the 22 hour MLT sector (i.e., 0.7 hour MLT apart from the Kotel'nyy station) at invariant latitudes higher than 68°. Polar UV data for the period just following the substorm onset are given in Plate 1. The first auroral intensification lasted only until ~1253 UT, Kotel'nyy being located under the auroral bulge. Around 1254:30 UT, Polar UV images display another more intense breakup (not shown). In Plate 1, Polar UV measurements some 2.5 min later (1256:38 UT) exhibit a well-developed auroral bulge. Plate 1 also gives the Interball projection at ionospheric heights (blue crosses). Note that the level of ionospheric UV emissions was low during the first breakup, ~40 photons $(cm^2\ s)^{-1}$. The second auroral activation was related with a further intensification of Pi2 pulsations at Kakioka (Figure 1). Plate 2 presents electron and proton energy-time spectrograms measured by Interball together with the deviation between the onboard measured magnetic field and the IGRF model. In this Figure, crossing of the auroral bulge is first noticeable at ~1240 UT (i.e., immediately after the substorm onset), when the electron spectrometer detects enhanced energetic electron fluxes (several keV) originating from the plasma sheet. Between 1241:25

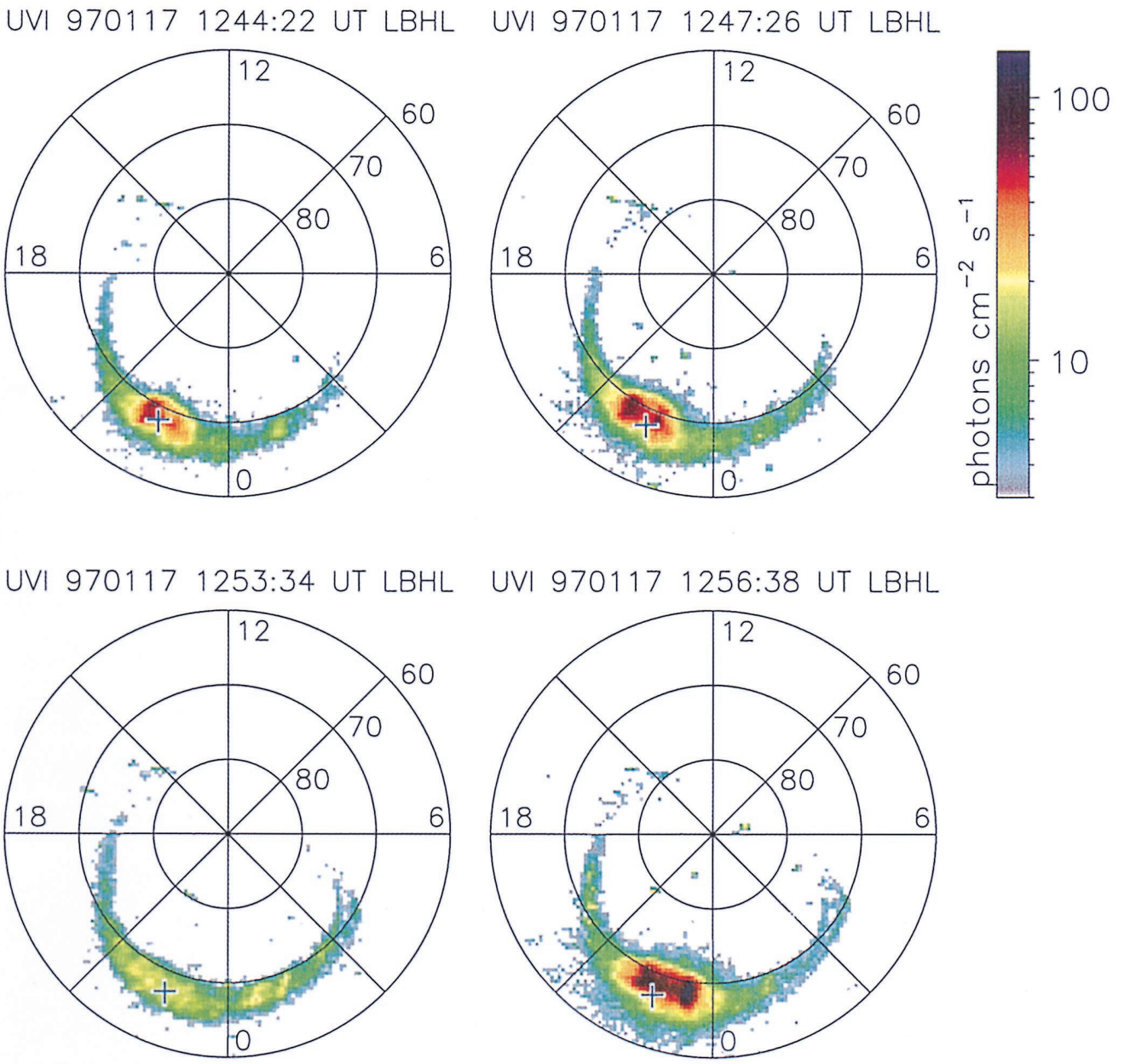

Plate 1. Selected sequence of Polar UV images, on January 17, 1997, in an invariant latitude, magnetic local time frame. The images are taken in the LBHL band near 1300 Å. The blue cross gives the projection of Interball-Auroral to ionospheric altitude (100 km).

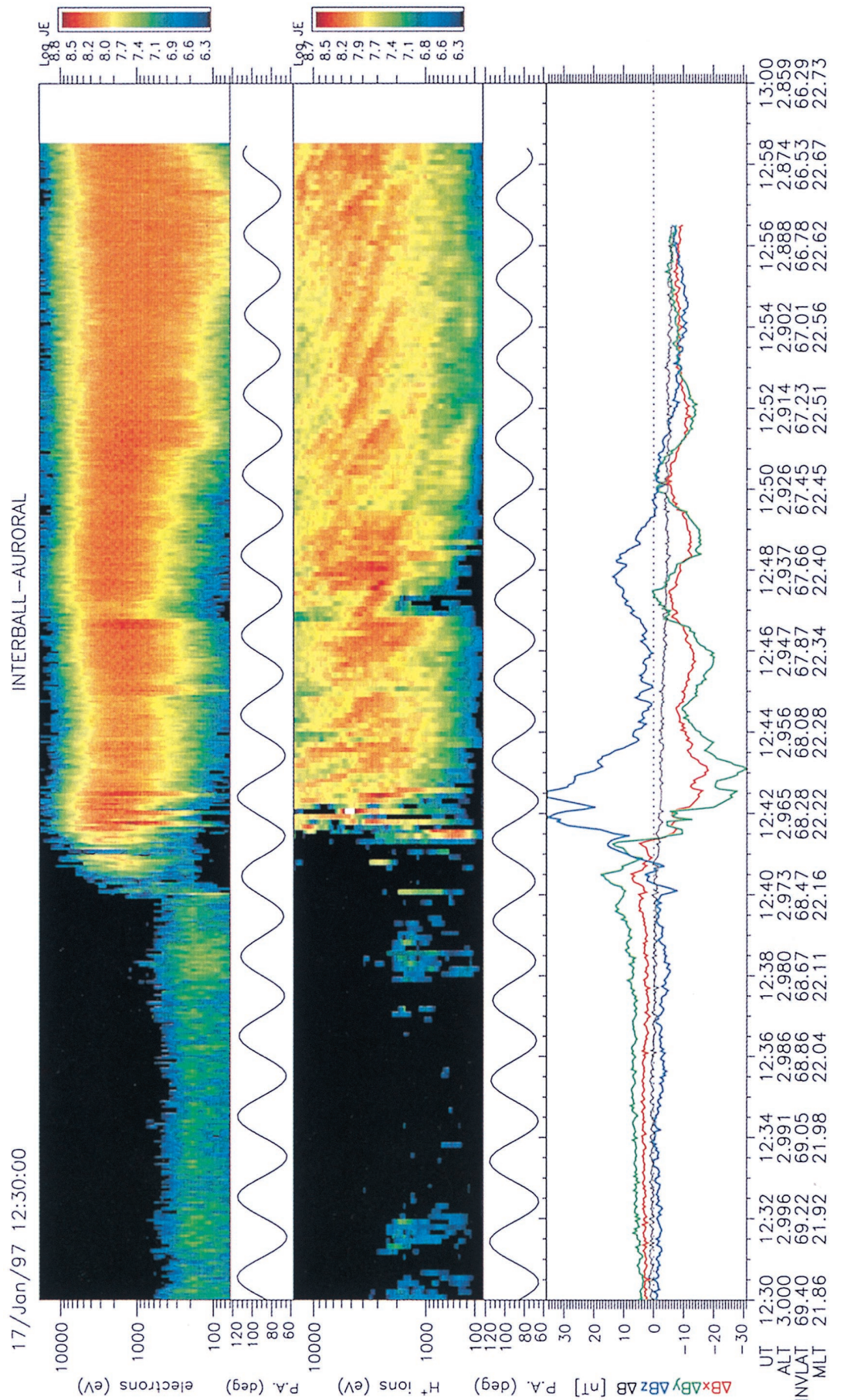

Plate 2. January 17, 1997, Interball-Auroral data between 1230 and 1300 UT. From the top to the bottom: electron energy-time spectrogram (energy fluxes are coded accordingly to the left color scale), electron pitch angle, proton energy time spectrogram and pitch angle, variations of the GSM component of the magnetic field relative to the IGRF magnetic field model.

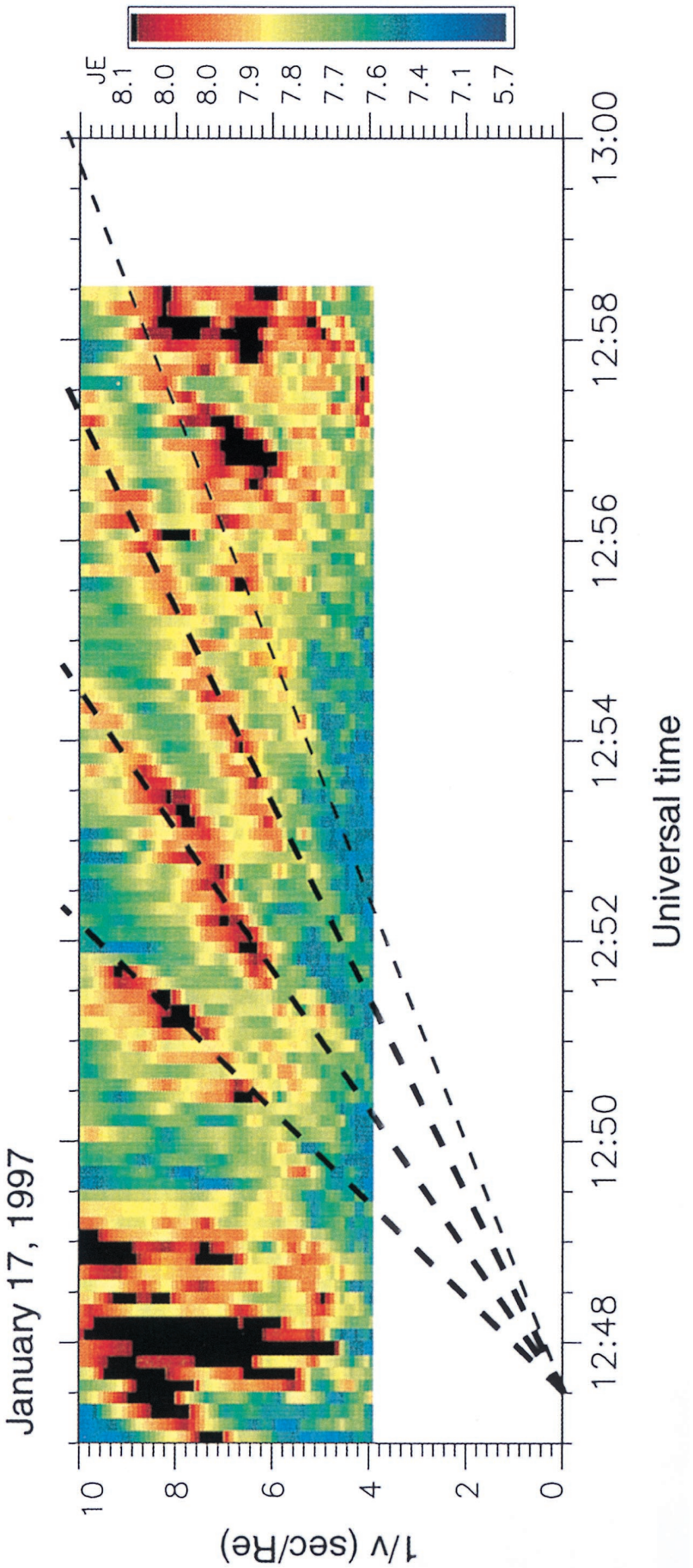

Plate 3. Inverse velocity (s/R_E) versus time spectrogram for the period 1247:00 to 1258:30 UT on January 17, 1997 (see Plate 2). The converging dashed straight lines, fitting the ion traces, correspond to the expected dispersion caused by time of flight effects of bouncing ions. The injection time deduced from this fit is ~1247:30 UT, in good agreement with the computation results presented in Figure 3.

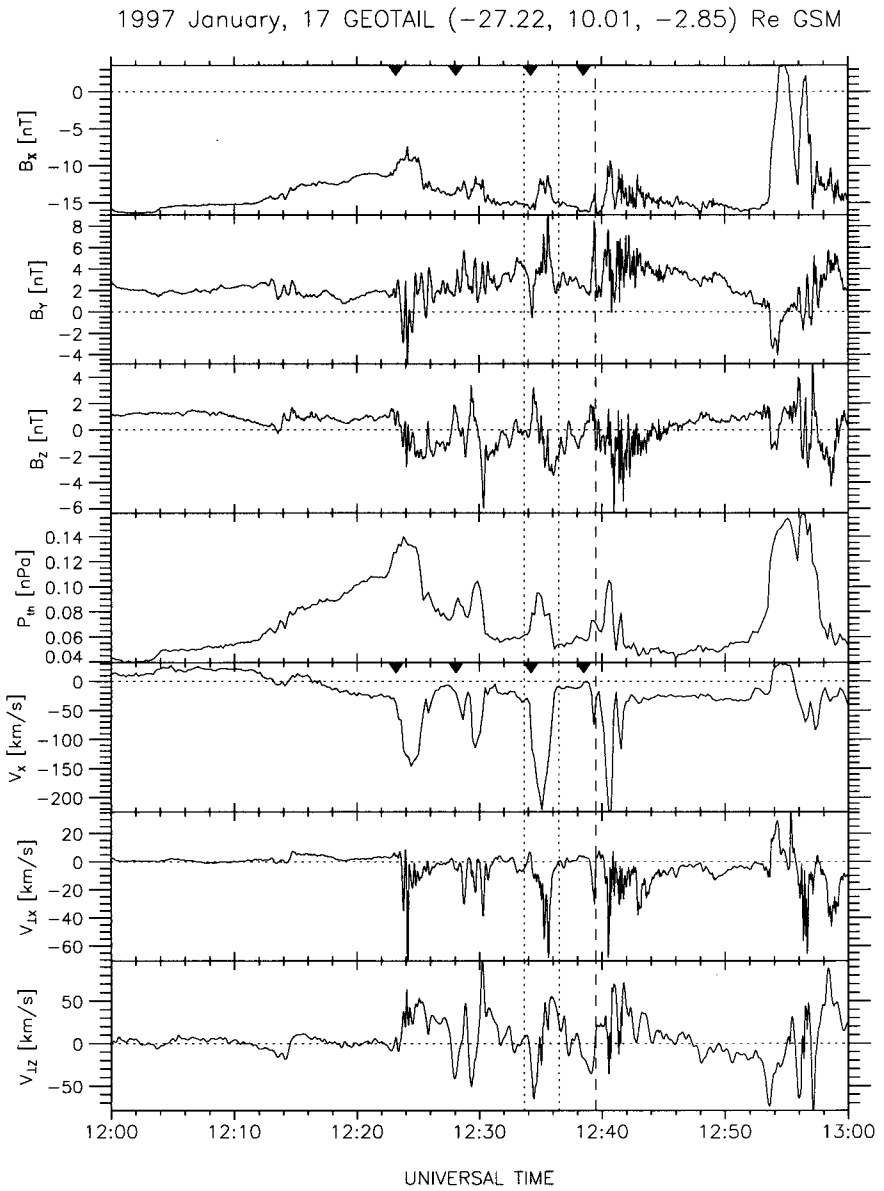

Figure 2. January 17, 1997, Geotail data from 1200 to 1300 UT. (top to bottom) The GSM X, Y, and Z components of the magnetic field, the ion thermal pressure, the GSM X component of the plasma velocity, the GSM X and Z components of the ion velocity perpendicular to the magnetic field. The two vertical dotted lines indicate the onset and end of a fast tailward plasma flow. The vertical dashed line gives the substorm onset time deduced from Pi2 pulsations at Kakioka (Figure 1). The black arrows mark successive short-lived intensifications of a bright spot of UV emissions detected from UV images from Polar in the 22–22.5 hour MLT sector, before the substorm onset.

and 1242:00 UT, discrete electron structures are seen with pitch angles from 70° to 110°. From ~1241:30 UT, discrete proton structures are observed together with the electron fluxes enhancements. At 1241:30 UT an upflow of ionospheric protons at pitch angles of ~110° is also recorded. After 1242:30 UT, energy dispersed structures of ions appeared with two distinct slopes: (1) high and nearly identical slopes before 1246:30 UT, and (2) softer and decreasing slopes after 1249:30 UT. Changes in both electron and proton fluxes between 1246:45 and 1249:30 UT are related to an intensification of the auroral surge near the satellite ionospheric footprint (Plate 1).

Beginning with the first electron flux enhancement, the magnetic field measured onboard Interball shows well-developed oscillations with a period of ~180 s. The ΔB of the waves is nearly zero (Plate 2). A wave analysis in a frame with one component aligned with the mean magnetic field (not shown here) indicates that the field-aligned component of the wave is ~0 and the hodograph shows a left-handed polarization with a wave amplitude of ~15 nT. These characteristics indicate that they are shear Alfvén waves propagating quasi-parallel to the background magnetic field toward the ionosphere. Superimposed on these oscillations higher-frequency waves can be seen (T ~40 s). These latter oscillations are clearly related to the electron flux enhancements between 1240:00 and 1242:40 UT. These waves have the same characteristics ($\Delta B = 0$, left-handed polarization) than the lower-frequency ones. As for the

longer-period oscillations, they show significantly weakening when the satellite reaches low latitudes.

During this event, Geotail was located in the midtail, at $X_{GSM} = -27.6\ R_E$, $Y_{GSM} = 8.4\ R_E$, $_{GSM} = 2.2\ R_E$. The satellite invariant latitude was ~70°, and the magnetic local time of its ionospheric projection was 21.9 MLT. Geotail was thus located inside the substorm UV activation seen from Polar. As displayed in Figure 2, the satellite was in the south plasma sheet ($Bx < 0$). During the southward interplanetary magnetic field (IMF) episode (Figure 1) and before substorm onset, a decrease of the Bx component of the magnetic field can first be seen in Figure 2 (from ~1203 UT). The magnitude of the total magnetic field is nearly that of the Bx component and clearly follows the variations of the plasma thermal pressure. This is attributed to diamagnetic effects. A series of four tailward directed plasma flow bursts with velocities between 120 and 240 km/s is subsequently noticeable between 1223 and 1243 UT. Each flow burst lasts for 1–3 min and the apparent recurrence time is ~5 min. During each flow burst, the magnetic field and the plasma velocity components present quite repetitive changes. For clarity in Figure 2, two vertical dotted lines mark the beginning and the end of the most intense burst which occurs before substorm onset. It can be seen that the main component of the velocity is directed tailward and that the Z component of the magnetic field has a clear bipolar variation (positive, then negative). The plasma velocity perpendicular to the magnetic field is smaller than the parallel one and also shows systematic changes. During the flow bursts, the X (GSM) component of the velocity perpendicular to the magnetic field is always directed in the anti-sunward direction while the perpendicular Z component of the velocity is anticorrelated with the Z component of the magnetic field (i.e., $V_{\perp Z}$ is negative when Bz is positive and turns positive when Bz becomes negative). These variations are in good agreement with the encounter of hot plasma bubbles or plasmoids convecting tailward. A possible interpretation is that these plasma and field structures are produced by partial disruptions of the cross-tail current occurring earthward of the satellite or by reconnection events, as proposed for similar observations by *Nagai et al*. [1997]. Note that the last tailward flow burst occurs from ~1239:40 UT, i.e., very close to the substorm onset time as identified from Pi2 pulsations at Kakioka (Figure 1). Finally, from ~1253:40 UT, a major change of the Bx component can be seen with two positive excursions indicative of neutral sheet encounters. These encounters possibly linked to expansion/flapping motions of the plasma sheet are closely related in time with the second intensification of the substorm recorded by the Polar UV camera at ~1254 UT.

The successive plasmoids encountered before the substorm can be directly related with the auroral activity monitored by the UV camera onboard Polar. Each plasma flow burst corresponds to a slight intensification of the UV emission localized in a spot located in the 22–22.5 MLT sector. The occurrence time of these weak electron precipitation enhancements are indicated by arrows at the top of Figure 2. Note finally that weak Pi2 pulsations were detected at Kakioka from 1229 UT, that is before the 1239 UT onset (Figure 1).

The energy dispersion of protons detected by Interball after 1249 UT (Plate 2) are strongly reminiscent of time of flight effects of bouncing ion clusters as originally reported by *Quinn and McIlwain* [1979] from equatorial measurements at 6.6 R_E. In order to test this hypothesis, we performed trajectory calculations backward in time in three-dimensional (3-D) magnetic and electric fields. These fields were represented by the *Tsyganenko* [1989] model (with appropriate dipole tilt) and the ionospheric electric potential distribution of *Volland* [1978] (for the details of the model, see *Delcourt et al*. [1989]). We sampled 24 energy, time, and pitch angle data points corresponding to the energy dispersion structures seen between 1250 and 1257 UT and verified that the particles contributing to the dispersed structures where launched at the same time from the same point source in the magnetosphere. The dawn-dusk potential drop was determined from the semiempirical model of *Weimer* [1996]. The input parameters of the model (the By and Bz components of the IMF and the solar wind velocity) were taken from Wind. The *Tsyganenko* [1989] state was determined as the least disturbed field, in agreement with the Kp index for the period of interest. We found that the computations give similar results for a wide range of cross polar cap potential drops (up to ~100 kV) and weak differences were obtained using a Tsyganenko model with a higher level of magnetic activity. The results of these calculations are displayed in Figure 3. It is apparent from this Figure that the particles have been ejected at ~1247:30 UT, from the equatorial plane, at distances of ~7–8 R_E. The ejection time nearly corresponds to that when a surge intensification was detected by the Polar UV camera close to Interball footprint (Plate 1). Particles forming the energy dispersed structures have been

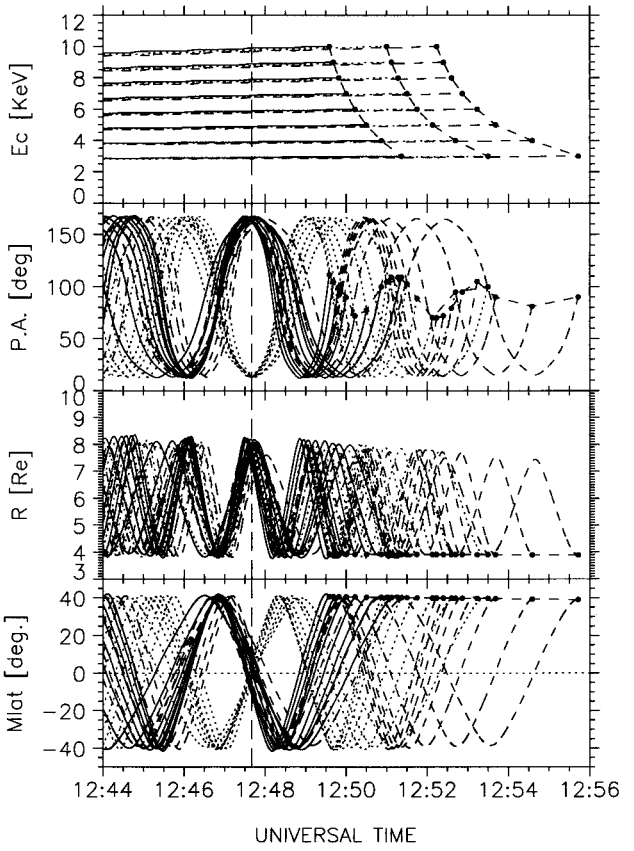

Figure 3. Backward computations of the ion energy dispersed structures seen after 1249:30 UT in Plate 2. Twenty-four energy and pitch angle points are being traced backward in time, starting from the dots. From top to bottom, the ion energy, pitch angle, radial distance, and magnetic latitude. Note the focal point at 1247:45 UT shown by a vertical dashed line.

ejected both toward the northern and southern hemispheres. The first trace, beginning at ~1249:30 UT corresponds to particles ejected toward the southern hemisphere, whereas the second trace involves particles ejected at the same time toward the northern hemisphere and bouncing once before reaching Interball. The third trace, made of particles ejected toward the south and bouncing twice is the echo of the first structure. These results are further supported by the fact that when displayed in a inverse velocity-time diagram, ion traces appear as straight lines and converge toward the computed injection time consistently with simple time of flight dispersion (Plate 3). Thus, as initially shown by *Quinn and McIlwain* [1979] at 6.6 R_E and by *Hirahara et al*. [1996] at auroral altitudes, the energy dispersion results here from different ion times of flight following a single injection from the inner magnetosphere (~8 R_E).

Using available LANL geostationary data, we verified that no injection of electrons or ions (with energies higher than 50 keV) were recorded at 6.6 R_E during this sequence of auroral substorm. Concerning the tailward jets of plasma seen onboard Geotail, it should be noted that earthward convection surges in the equatorial magnetosphere have been reported up to 10 R_E even during quiescent periods as in the present case ($Kp = 0_0$) [see *Nishida et al*., 1997].

If injections were slowly propagating from low latitudes (close to the Earth), near the first substorm onset, to high latitudes (farther from the Earth) as the substorm progresses, we would expect the computed injection time of the ion cluster event to coincide with the onset time, i.e., ~1239 UT instead of 1247:30 UT. This discrepancy raises questions regarding the time sequence and recurrence of the ion injections. The Geotail observation, at ~29 R_E, of bursty tailward flows before and at substorm onset provides evidence that the substorm process is affecting a wide region of the magnetospheric tail.

Finally, it is apparent from Plate 2 that before encountering the bouncing ion clusters, Interball records repeated keV proton structures at high latitudes (~1242:30, 1244:00, 1243:00 UT, etc.). Here the slopes of these structures are nearly identical, which precludes a bounce effect as described above. This type of sporadic injections is frequently observed by Interball near the auroral bulge poleward boundary. However for the January 17, 1997, event, the time resolution of the measurements does not allow detailed analysis of these structures and different passes will be considered in the next section.

3.2. Multiple Sporadic Ion Injections Near the Poleward Boundary of the Northward Expanding Bulge

Interball data reveal an unexpectedly high rate of occurrence of time of flight dispersed ion structures (TDIS) during substorms. Some of these structures are measured near or at the substorm onset time. However, the probability for the satellite to be located at the surge front near the time of onset is low. In fact, it appeared that throughout the expansion phase, this type of dispersed ion structures are detected inside the auroral bulge as well, which explains the high-detection probability. Some of these ion dispersed structures show bounce effects as in the preceding example, mostly at low latitudes. Nonbouncing structures are more characteristic of the high-latitude parts of the bulge.

3.2.1. October 10, 1997. In order to present typical data obtained in the midnight sector during disturbed times we show in Plate 4 electrons, ions (H^+ and O^+) and magnetic field observations achieved on October 10, 1997 [$Kp = 5-$], at high latitudes during a multiple substorm sequence. The data corresponding to the time interval 1825–1855 UT are presented in a format similar to that of Plate 2. However, oxygen fluxes here exceed the background level so that the oxygen energy-time spectrogram has also been added (third panel from the top). The general pattern in Plate 4 is quite similar to that of Plate 2. Onboard the satellite, the poleward border of the surge as identified from electron energy flux enhancements is detected around 1829 UT. About 2 min later the satellite encounters the first precipitating ions with a clear proton energy dispersion in the range 4–14 keV. Simultaneously, low energy (below ~1 keV) H^+ and O^+ ion conics are detected. As in the case illustrated in Plate 2, the magnetic field components displayed oscillations with a period close to 180 s and superimposed higher frequencies ($T \sim 40$ s) strong fluctuations near the poleward edge of the surge (see Plate 5). A clear time of flight dispersion is also apparent in the oxygen energy-time spectrogram after 1839 UT. Note that the electron spectrogram exhibits temporary intensifications, particularly near the surge poleward boundary. However, the slow spin rate of the satellite does not allow to resolve the electron pitch angle distributions. After the surge encounter, additional ion and electron flux enhancements are detected around 1849 UT, while the satellite is traveling toward lower latitudes.

To put these observations into perspective, Figure 4 and Plate 5 present IMAGE magnetograms and Polar UV images corresponding to this Interball pass. The IMAGE chain with a magnetic local time of 2200 at 1830 UT (0100 MLT from Interball) showed a substorm onset around 1812 UT at Bear Island (BJN) station located at an invariant latitude of ~71.33°. At lower latitude (SOR), the variation of the X component of the magnetic field reveals the simultaneous development of a substorm recovery (Figure 4). At 1830 UT, Interball footprint was located in the evening sector, at a magnetic local time of 23.02 and an invariant latitude of 71.14°, i.e., close to those of Bear Island (BJN) and Hopen Island (HOP). Selected Polar UV images are displayed in Plate 5 for the period 1828:19 to 1835:27 UT. The first picture taken 16 min after substorm onset shows a well-developed bulge with Interball located close to its northward boundary. At that time, Interball records enhanced electron precipitation but no ion flux in the spectrometer energy range ($E \leq 14$ keV). The second image is given at 1832:23 UT. The bulge northward boundary is here located poleward of Interball which now detects keV proton injections. The third image in Plate 5 is for 1835:27 UT. The bulge has moved to the north and reached a latitude of ~75°. Well-defined ion injections are detected onboard Interball. The accuracy of the relative latitudinal positions of the Polar data with respect to those of Interball is estimated to ~1°. This accuracy mainly depends on the orbit determinations, and on the magnetic field model used to project the Interball position into the ionosphere. Another source of error also comes from the wobble of the Polar platform which is dawn-dusk and will shift in this direction any boundary by the equivalent of ~2.5° MLT.

At geostationary orbit available data (not shown) come from the LANL 1994-084 satellite, located at MLT = UT + 7 hours. A series of flux dropouts and injections of energetic particle ($E > 50$ keV) were observed from ~1715 UT, in close association with a ~500 nT electrojet intensification seen at SOR (INVLAT = 67.27, $L = 6.7$). These injections occur until 2000 UT. However, LANL was located in the morning sector

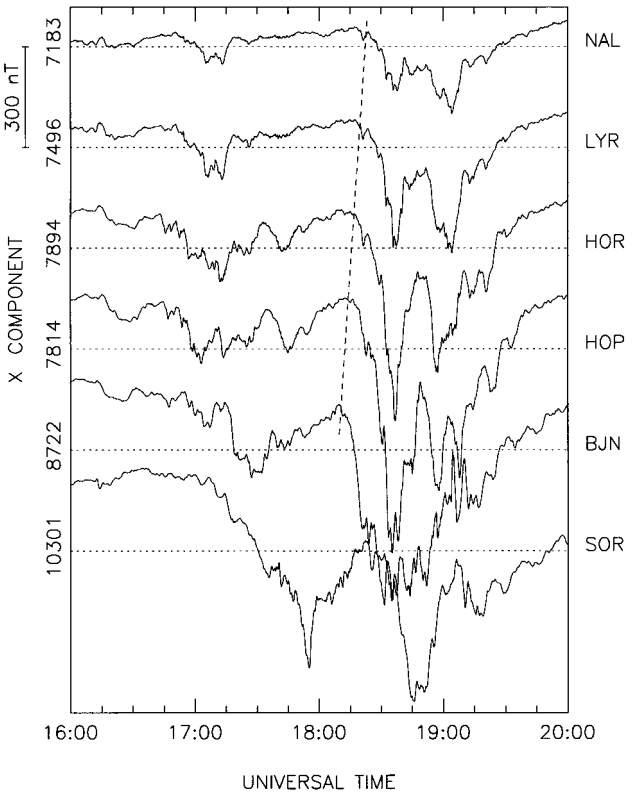

Figure 4. Horizontal X components of the geomagnetic field at the most poleward stations of the IMAGE magnetometer network on October 10, 1997. The magnetic local time of the chain is MLT ~ UT + 3.5 hours. The stations are Ny Ålesund-NAL (INVLAT = 76.07°), Longyearbyen-LYR (75.12°), Hornsund-HOR (74.02°), Hopen Island-HOP (72.93°), Bear Island-BJN (71.33°), and Sørøya-SOR (67.24°). The dashed curve indicates the progression toward the north of the westward electrojet.

when Interball crossed the auroral bulge near local midnight so that direct detailed comparison is not possible.

As in the January 17, 1997, case, we performed trajectory calculations backward in time to estimate the time when the ions observed close to the northern border of the bulge were ejected from the equatorial magnetosphere. However, here H^+ ions do not show bounce effect but nearly parallel energy-time dispersions between 1835 and 1845 UT. The energy-dispersed structure of O^+ was also used to estimate the injection time. The results of the computations are shown in Figure 5 together with projection into the noon-midnight meridian plane of the model field line connected to the satellite. A cross polar cap potential drop of 80 kV was chosen and proven to only have a weak effect (the particles keep an almost constant kinetic energy) on the computations as the magnetic field for any configuration of the model is very stretched, given the high latitude of the satellite. The use of a realistic magnetic field model essentially allows us to account for pitch angle unfolding (under magnetic moment conservation) due to the Earth magnetic field and to disentangle energy/pitch angle variables. It can be seen in Figure 5 that within each dispersion structure (including the O^+ one) the particles from each single trace have been ejected nearly simultaneously from regions located near the magnetic equatorial plane: (1) at ~1833:40 for the first H^+ structure, (2) at ~1835:00 for the second, and (3) also at ~1835:00 UT for the O^+ one. In all cases, the particles are found to come from the midtail, from 18 (O^+) and 27–35 R_E (H^+), the magnetic latitude of the source being ~7°–10°. Note, however, that for hydrogen some radial dispersion is visible. As noted above, varying the models does not change the results strongly. In this October 10, 1997, case, the absence of bouncing clusters likely follows from stretching of the magnetospheric field line in the midtail which leads to the violation of the ion first adiabatic invariant. Chaotization of the motion and pitch angle scattering as the particles return to near equatorial regions after mirroring at low altitudes prevent the formation of a dispersed pattern as in Plate 2. Starting from 1850 UT, when Interball has reached latitudes of the order of 69.2° other hydrogen- and oxygen-dispersed structures are detected and here one must consider the possibility that these ions originate from the ionosphere as suggested by *Delcourt et al.* [1999].

3.2.2. December 22, 1996. Plate 6 shows Polar UV data together with Interball projection at 100 km along the field line, for the period 1640–1714 UT on December 22, 1996 ($Kp = 2_+$). Interball crossed the eastern poleward border of an auroral surge at ~1639–1640 UT and the combined displacements of the satellite and of the surge subsequently moved Interball to the central part of the intense auroral precipitation. At 1714:13, Interball is located deep into the bulge. Note that the auroral activity is now very enhanced in the afternoon sector. Electron, hydrogen, and magnetic field measurements performed during this pass are displayed in Plate 7 (no precipitating oxygen ions were recorded). Interball reached the auroral bulge at ~1639 UT, as indicated by electron energy flux enhancements. A strong outflow of hydrogen ions is first observed when the instrument is looking at pitch angles in the upgoing direction (1640 UT). Afterward, a series of energy-dispersed ion structures is noticeable throughout the crossing of the auroral zone, up to 1725 UT. Low-frequency waves with periods ~180 and ~40 s are once again detected, the largest amplitudes occurring at the northern border of the surge. Note also the repeated dropouts in the electron and ion fluxes ($E > 2$ keV) which could be due to intermittent spacecraft reentry into the polar cap, for example, at ~1657 UT. At 1639 UT, i.e., when crossing the bulge north boundary, the satellite (INVLAT = 71.9°, MLT = 23.6) was located close to the 210MM magnetometer chain, ~1° north of Kotel'nyy (MLT = 24.5 at 1638 UT). The horizontal magnetic field component of this station and that of Tixie are displayed in Figure 6 together with the high-energy electron fluxes measured onboard LANL 1994-084, which is located at the same local time as Interball at 1638 UT (MLT = 23.5). A negative bay at Kotel'nyy at ~1630 UT preceded the Interball encounter with the surge by 9 min. At 1630 UT, LANL 1994-084 also displays an electron injection extending from 50 to 315 keV. Later between 1638 and 1730 UT a succession of sporadic injections in the energy range 50–150 keV was detected at geostationary orbit. However, there is no clear relationship between these high-energy electron injections seen at 6.6 R_E and sporadic ion-dispersed structures recorded by Interball, with the exception of the strong injection viewed from 1712 UT by LANL, which may be related with the ion flux enhancements seen by Interball immediately after.

As shown in Figure 7, during this event, Geotail was located in the midtail at ~30 R_E in the morning sector (~0200 MLT). Its computed invariant latitude is 72°. Note that the east part of the auroral bulge near 1640 UT in Plate 6 extends to the

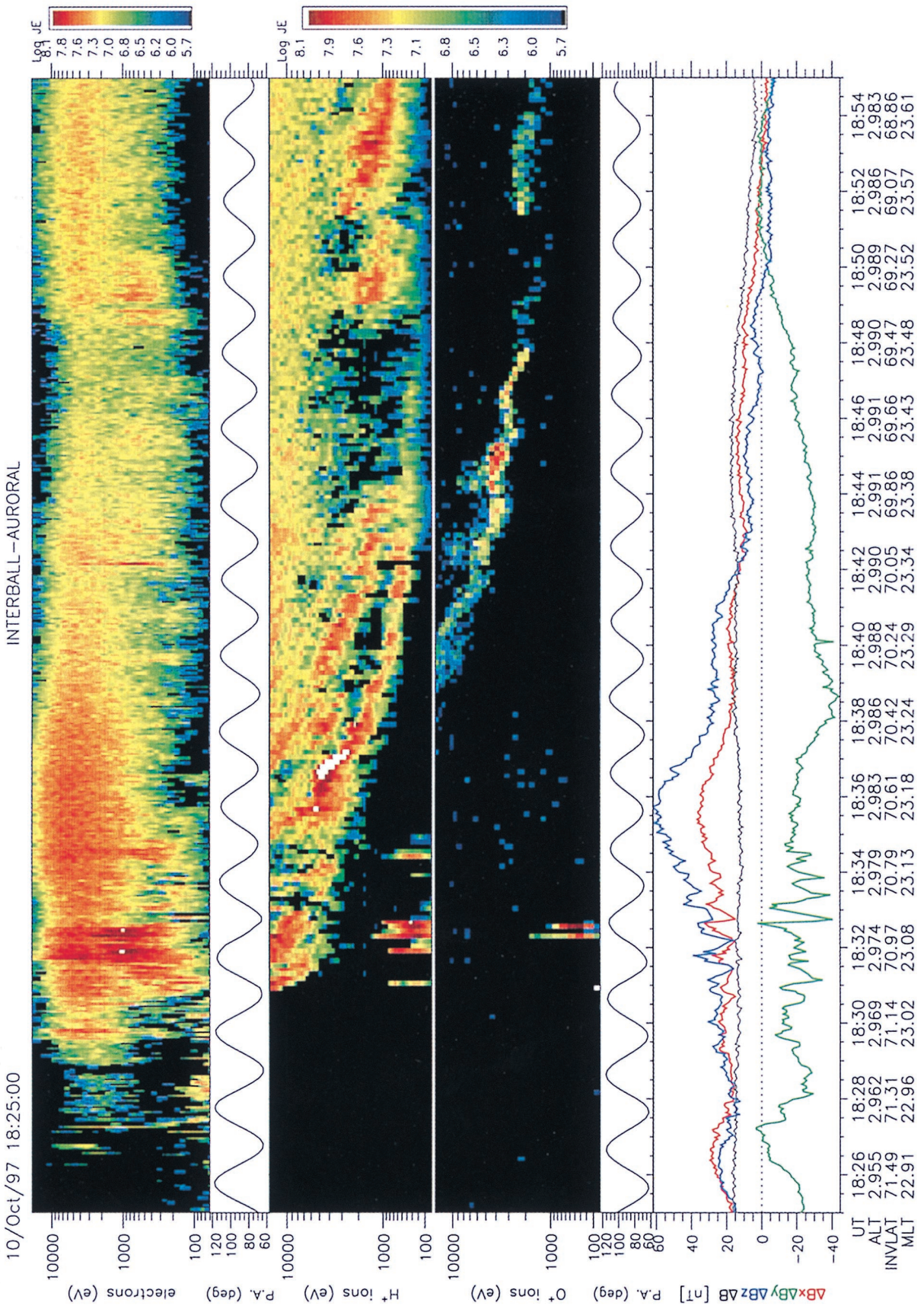

Plate 4. October 10, 1997, Interball-Auroral data. The presentation is similar to that of Plate 2, except for the addition of the oxygen spectrogram (third panel from the top).

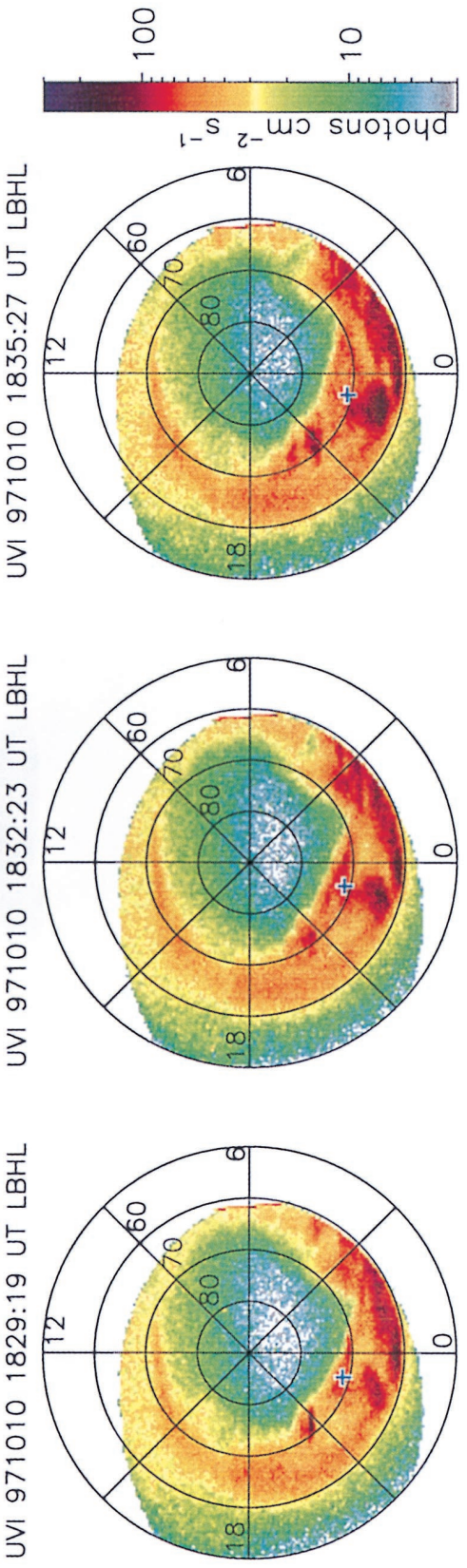

Plate 5. UV image in the LBHL band from Polar in an invariant latitude and magnetic local time plot at 1829:19, 1832:23, and 1835:27 UT on October 10, 1997. The projection at 100 km altitude along the magnetic field line of Interball is shown by a cross.

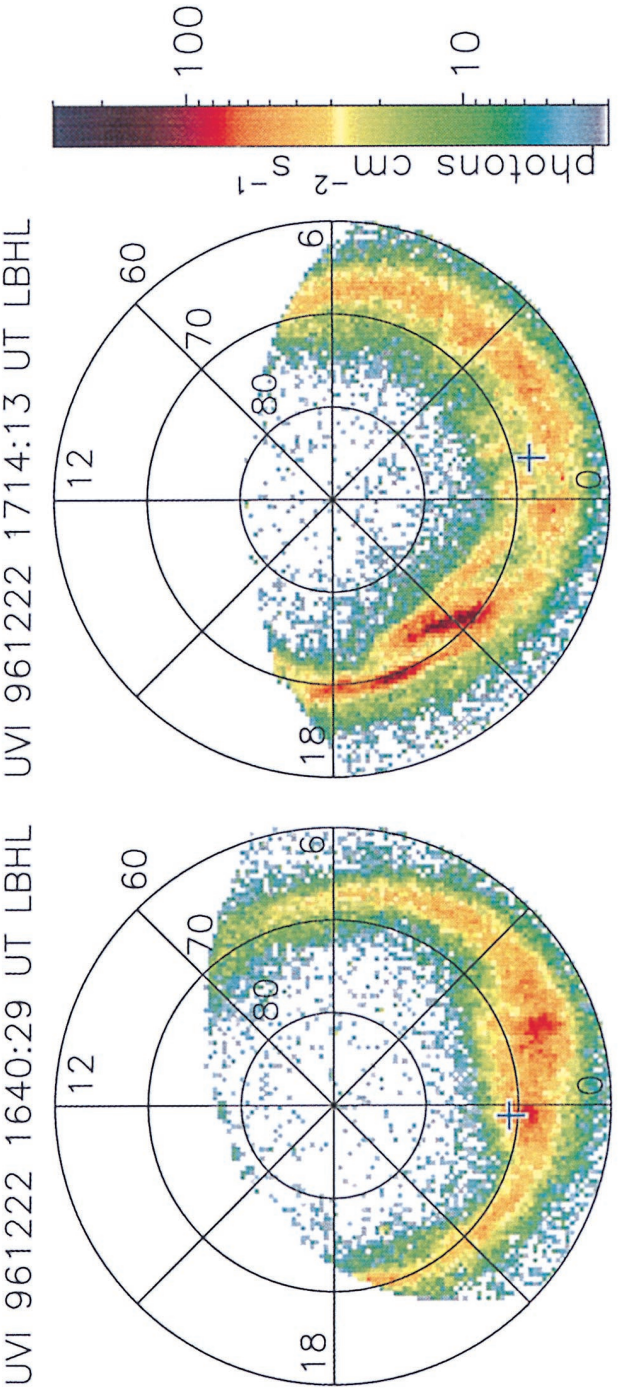

Plate 6. December 22, 1996, UV data from Polar in the LBHL band. The presentation is similar to that of Plate 5. The Interball-Auroral projection at 100 km height is shown at 1640:29 and 1714:13 UT by blue crosses.

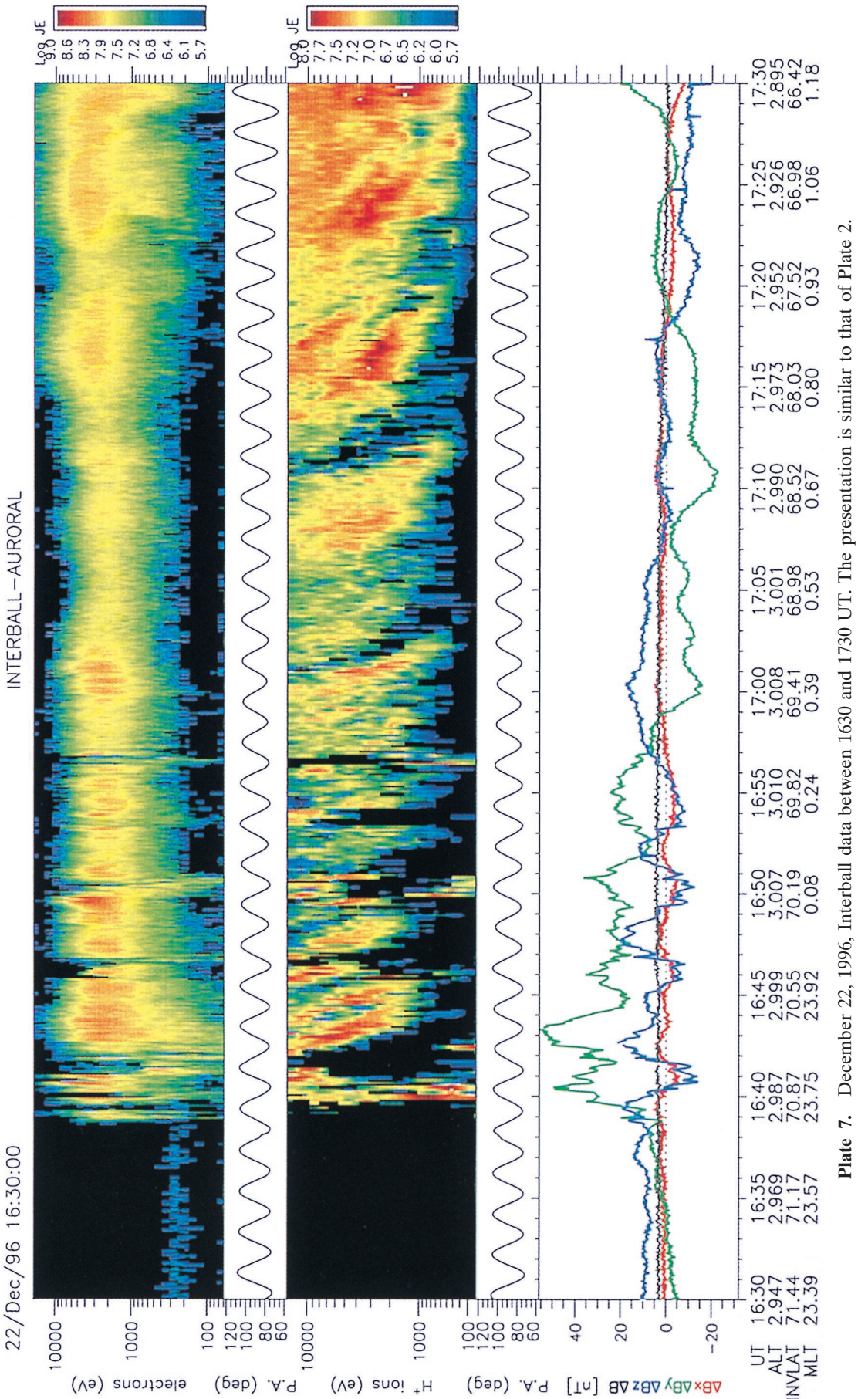

Plate 7. December 22, 1996, Interball data between 1630 and 1730 UT. The presentation is similar to that of Plate 2.

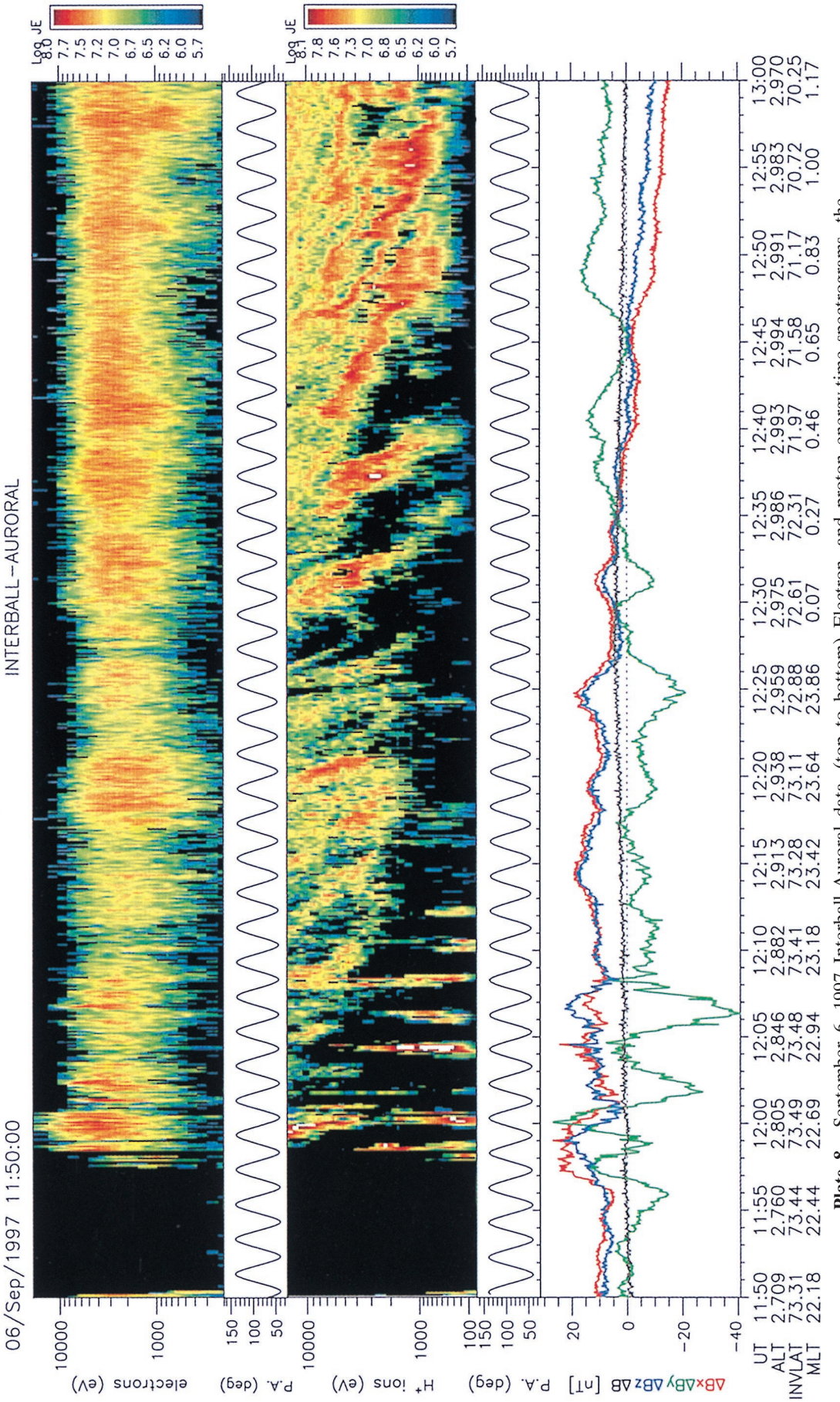

Plate 8. September 6, 1997 Interball-Auroral data. (top to bottom) Electron, and proton energy-time spectrograms, the deviations of the GSM X, Y, and Z component of the magnetic field relative to the IGRF magnetic field model.

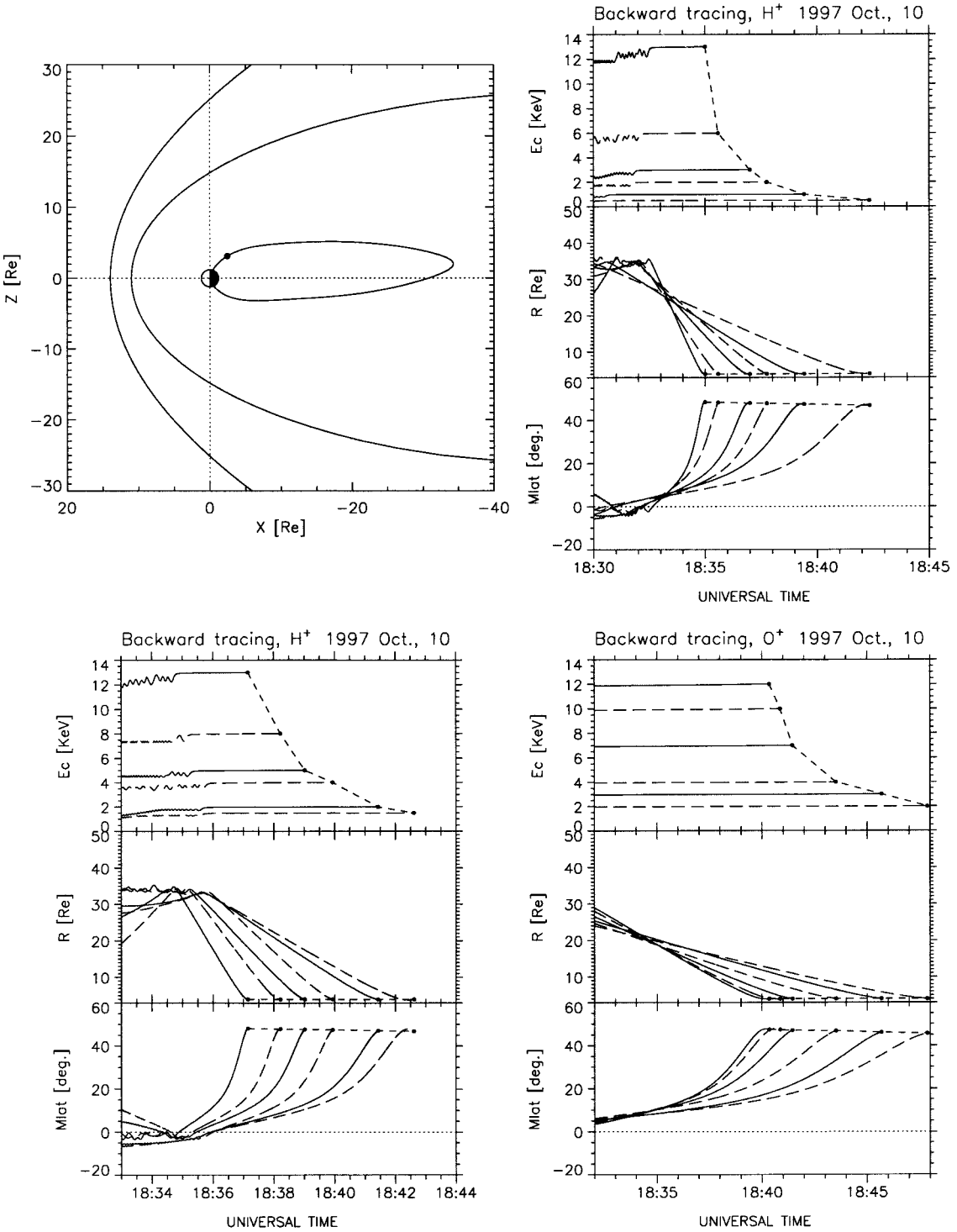

Figure 5. (top left) Projection into the noon-midnight meridian plane of the magnetic field line passing by Interball on October 10, 1997, at 1835 UT. Upper right, trajectories computed backward in time for the H^+ dispersed structure starting at ~1835 UT. (bottom left) Same for the H^+ structure seen at 1837 UT. (bottom right) Same for the O^+ dispersed structure starting at 1840 UT. Each trajectory plot gives the ion kinetic energy, radial distance, and magnetic latitude.

morning sector up to local times corresponding to the Geotail position. Starting at ~1637 UT, i.e., close to the time when Interball crossed the north and west border of the auroral surge, Geotail passed from the southern lobe to the plasma sheet where beams with an earthward velocity reaching 550 km/s were measured. These beams were recurrently detected between 1637 and 1712 UT in association with significant increases of the plasma temperature. The persistence of the flow well into to the central plasma sheet can be deduced from the high-velocity flow event encountered during the time period

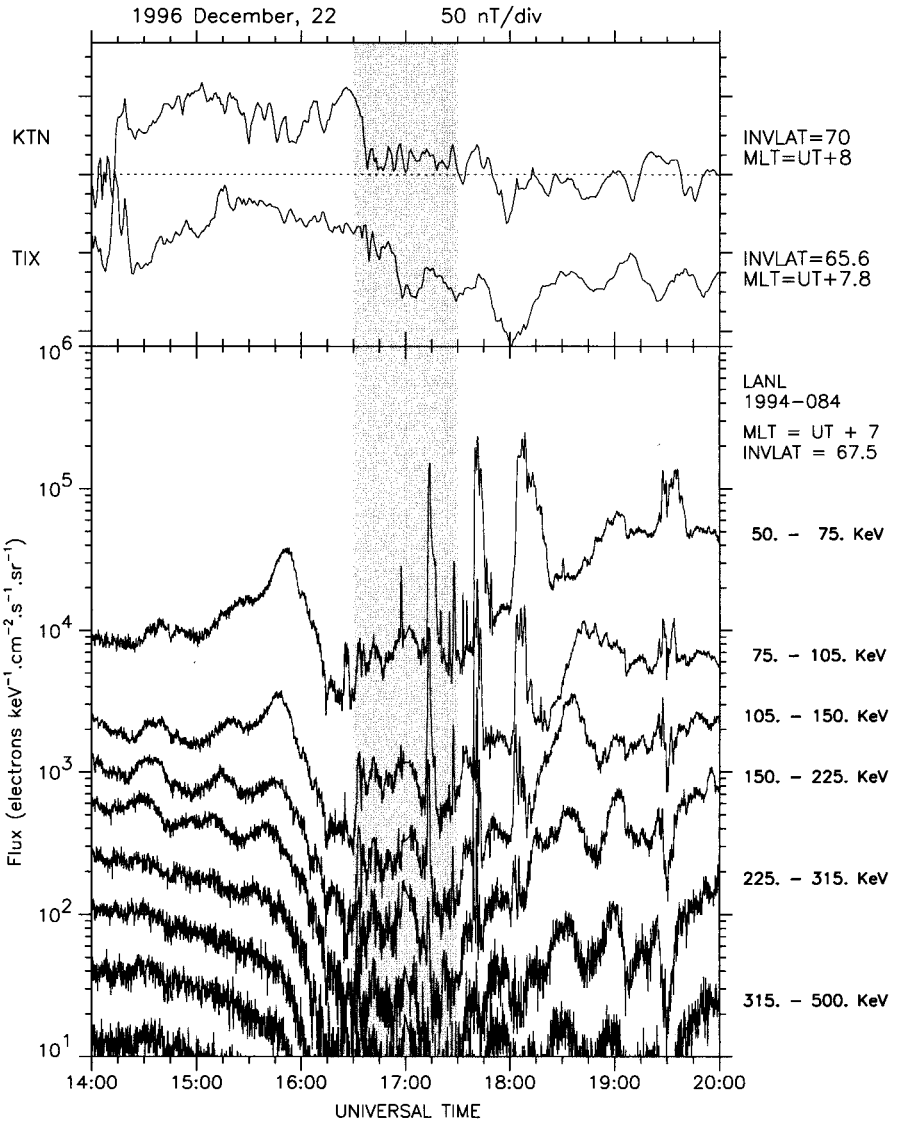

Figure 6. December 22, 1996, ground and geostationary data. Top, the horizontal component of the geomagnetic field at Kotel'nyy and Tixie (210MM chain). Bottom, the energetic electron flux detected onboard the LANL 1984-084 geostationary satellite located 0.8 hour MLT eastward of the 210MM magnetic meridian chain. The gray area delineates the time period corresponding to the Interball data presented in Plate 7.

1705 to 1712 UT when the velocity is higher than 400 km/s and the magnetic field *Bx* component varies between +1 and −5 nT. The highest flow velocity was measured around 1652–1653 UT, reaching 800 km/s, well inside the plasma sheet as indicated by the small value of the magnetic field *Bx* component. Note that during the period 1630 to 1730 UT, the *Bz* component of the magnetic field was mainly positive. For this case, the sporadic and recurrent high-speed plasma flows directed earthward strongly suggest that Geotail was located earthward of an intermittent reconnection site in the more distant plasma sheet. Although there is no one to one correlation between the plasma sheet dynamical change as deduced from Geotail data and the succession of ion injections seen onboard Interball, the observations suggest that the bursty bulk flows have pseudo-periods of 1–5 min, very much like the ion injections into the auroral zone.

As in the preceding examples, we computed ion trajectories backward in time to estimate the ejection time from the equatorial magnetosphere. Figure 8 shows the results of these computations for two ion structures namely those observed at 1642 UT (INVLAT = 70.7°) and ~1700 UT (INVLAT = 69.41°) respectively. It can be seen in Figure 8 that the ions are injected ~1 min before their first detection by Interball, from radial distances of the order of 22 R_E in the former case and 18 R_E in the latter, i.e., from a region closer to the Earth than Geotail. Later, when Interball is located more deeply into the surge, i.e., more equatorward, dispersed ion structures are still measured though with wider extension and a softer slope.

In this December 22, 1996, pass we cannot rule out the existence at low latitudes of ion clusters experiencing multiple bounces (INVLAT < 67.2°). There is an indication for such a possibility in Plate 7 after 1721 UT, when the dispersion signatures merge into a unstructured precipitation of plasma sheet ions. For the clearest high-latitude TDIS we have been

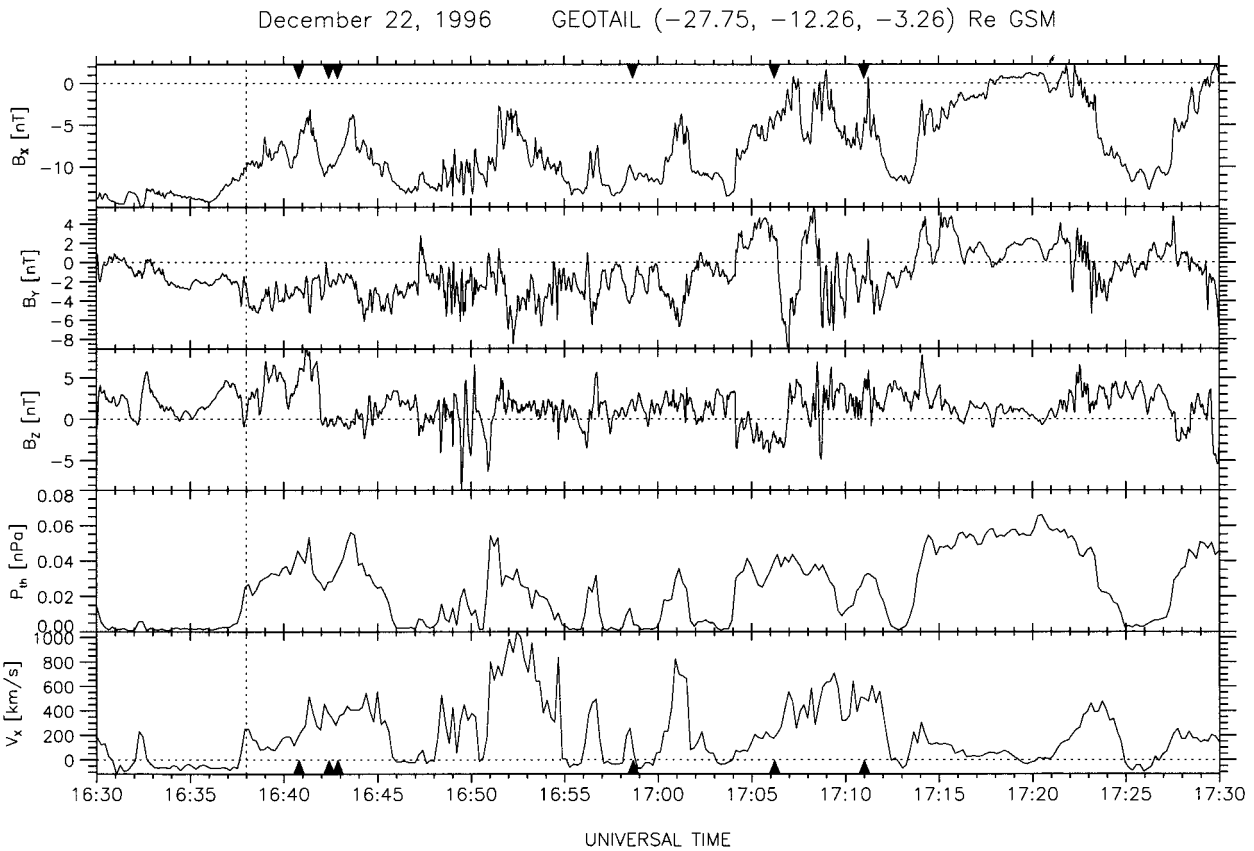

Figure 7. December 22, 1996, Geotail data. The presentation is similar to Figure 2. However, only the GSM X component of the plasma bulk flow is given. The vertical dashed line marks the time when Interball crossed the poleward border of the auroral bulge. The arrows indicate the computed injection times of clear TDIS deduced from Interball data (see text).

able to estimate the injection times and to compare them with the Geotail data displayed in Figure 7. This comparison suggests that injections occur for high-flow velocities and reduced magnetic field periods which could indicate sporadic reconnection events. However, the local time difference between Interball and Geotail leads us to consider these correlations with care. More extensive studies are needed.

3.2.3. September 6, 1997. This north to south pass of Interball with a surge encounter near 1158 UT ($Kp = 2_0, 3_-$) also displays a series of time of flight dispersed ion structures. These structures exhibit all the characteristic features generally observed by Interball at altitudes of the order of 20,000 km during substorms. However, in that case the northern boundary of the surge is crossed at a particularly high invariant latitude (73.5°). Near the surge poleward boundary, intense proton conics can be seen with energies up to 5 keV. From the pitch angle variation of these ions we can infer that the heating process is taking place at least up to altitudes of ~18,000 km, i.e., not far from the spacecraft. Starting around 1159 UT, clear high-energy dispersed hydrogen structures are detected. Later (after 1230 UT), the dispersion structures extend down to E ~1 keV. Note that on this pass the level of magnetic oscillations is high. Trajectory computations indicate that ions in the series of structures observed before 1240 UT are dispersed by time of flight effect and originate from the midtail, at distances of the order of 30 R_E. As already noted, at the highest latitudes, over the ionospheric heating region, the dispersion structures exhibit a low-energy cutoff around 2–4 keV and extend up to energies higher than the detector upper limit. In such cases, accurate backward computations are difficult. (However, the velocity^{-1}-time spectrogram (not shown) reveals that the structures have very similar slopes.) Different mechanisms may be invoked to explain the above low-energy cutoff. One is the deceleration of particles along the field line by parallel electric fields. Another mechanism is that the strong convection electric field does not allow connection between the low-energy part of the source and the satellite. The nature of heating processes in the equatorial plane may also be invoked. These topics clearly require further studies.

Finally, Plate 8 displays another feature of interest, namely a well-defined change of the TDIS slope after 1240 UT followed by their progressive mixing at lower latitudes. This results into a more uniform precipitation of hydrogen ions extending from ~200 eV to >14,000 eV when the satellite reaches invariant latitudes of ~70.5° at MLT = 1.1 MLT. The slope change at 1240 UT likely results from a bounce effect as ratio of the computed travel times for the 1234 and 1240 UT ion structures is of the order of 3.

4. Discussion

4.1. Two Types of Dispersed Ion Structures Associated With Auroral Bulges

We presented evidence for a new feature of auroral substorm, namely, the sporadic injection of ions from the plasma sheet throughout substorm expansion phases. Two types of

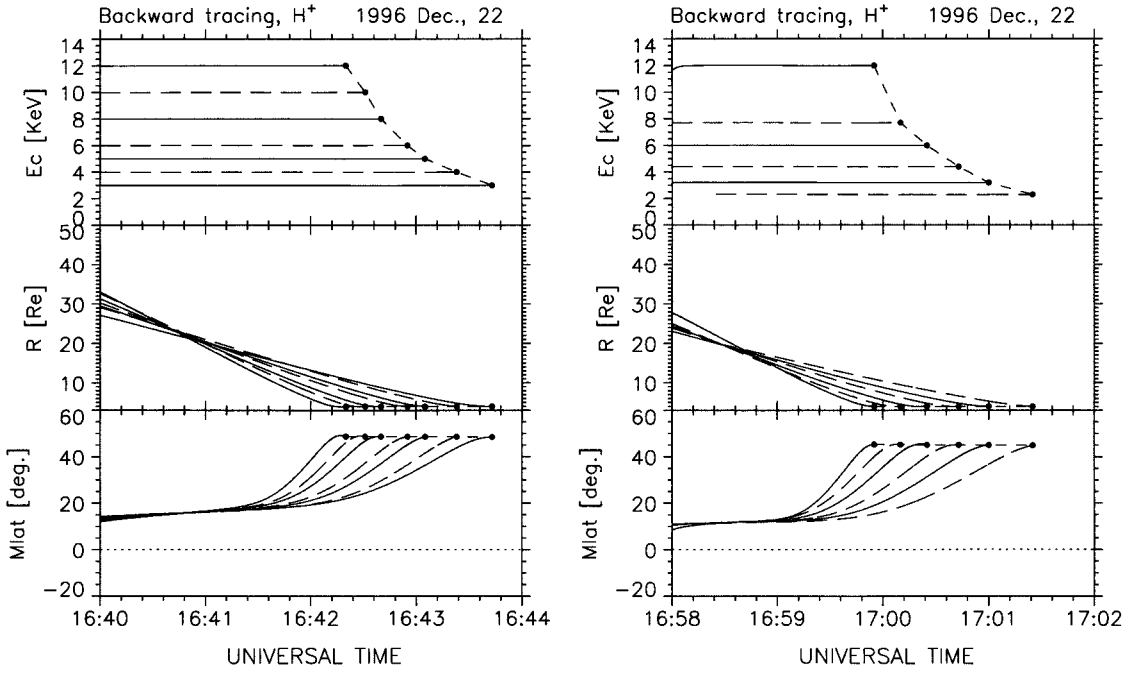

Figure 8. H^+ trajectories computed backward in time for the dispersed structures starting at (left) ~1642:18 UT and (right) ~1700:00 UT on December 22, 1996.

injections can be identified from Interball measurements at an altitude of ~3 R_E, above the auroral zone: (1) bouncing ion clusters similar to those observed by *Quinn and McIlwain* [1979] at geostationary orbit. Their source is found to be located in the nearly dipolar part of the plasma sheet, (2) nonbouncing, sporadic structures due to the time of flight dispersion of ions intermittently ejected from the midtail. In this latter case, we interpret the absence of bounces as the result of nonadiabatic pitch angle scattering when ions return to the equatorial plane.

These observations are new in the sense that we demonstrate the nonbouncing and recurrent dispersions are due to time of flight effect acting upon ions ejected from the plasma sheet (TDIS). This result is in clear contrast with previous analysis of velocity-dispersed ion structures (VDIS) made from low-altitude measurements by polar spacecraft, which conclude to either a very distant source and to predominant effect of the convection electric field [*Kovrazhkin et al*., 1987; *Bosqued et al*., 1993; *Elphinstone et al*., 1995; *Hirahara et al*., 1997] or to a single time of flight ejection followed by bounces in quasi-dipolar field lines [*Hirahara et al*., 1996]. By contrast convection electric field has a quite secondary role in the TDIS signatures related to auroral bulges reported here. The controlling factor simply is the different time of flight of ions with different energies. It must be stressed that a major substorm signature in geostationary data is particle acceleration and injection toward the inner magnetosphere. However, such satellites rarely coincide with the projection of the auroral bulge northern boundary, which generally lies tailward of them. Interball is systematically intersecting this border when traveling from dayside to nightside auroral zone, and thus it is well suited to examine the nature of ion injections. The Interball altitude near apogee allows it to stay for tens of minutes in this high-latitude region while low-latitude orbiting satellites quickly travel through it. Interball is accordingly better suited to resolve spatiotemporal effects. Finally, it must be stressed that both VDIS and TDIS are detected in the auroral regions. TDIS are restricted to the auroral bulge while VDIS have been reported over the entire evening sector, from 1800 to 0600 MLT, with no correlation with substorm phase [*Zelenyi et al*., 1990].

4.2. Sporadic Nature and Extent of Ion Injections

An important result concerns the sporadic nature of TDIS, their quasi period being of the order of 1–3 min near the poleward boundary of the auroral surge. It must be noted that such injections are observed during the expansion phase of substorms irrespective of the time delay from onset. This has important implications on the nature of the plasma sheet instability at work during a substorm. The instability should have the same recurrence time. This is also a strong indication that this process should be approximately invariant in the X direction, corresponding to its general tailward propagation (i.e., to northward propagation of the auroral surge). In other words as substorm progresses, successive regions of the tail should be affected by the same sporadic physical process.

Another important result is that injections are detected when the satellite is located inside the auroral surge as well. At first glance, this seems paradoxical bearing in mind the backward computations which show that each structure originates from a narrow domain in the equatorial magnetosphere. However, this localization directly follows from the sporadic nature of the injections and from the nearly unchanged satellite position during a single event observation. The fact that repeated TDIS are still detected when the spacecraft is immersed well inside the auroral bulge indicates that the process responsible for ion alignment with the magnetic field and subsequent detrapping must affect a wide range of radial distance in the equatorial magnetosphere or that this process rapidly propagates from the outer to the inner magnetosphere. However, the measurements presented here do not allow us to estimate the extent of the acceleration region. This issue is being ad-

dressed by *Sergeev et al.* [1999], who uses simultaneous space and ground observations. Further studies using correlated measurements from Interball-Auroral and Interball-Tail are also under way.

4.3. Related Low-Frequency Waves

The crossing of the poleward boundary of the auroral bulge systematically coincides with the detection of low-frequency waves. In this regard, it should be noted that a number of possible wave modes and harmonics may be excited during substorms: the shear Alfvén wave, the slow magnetosonic wave, and the fast magnetosonic wave, with their higher harmonics. We have chosen to work on ΔB values as compared to the IGRF model, whereas ∂B changes along the satellite orbit are indicative of field-aligned currents. Because Interball intersects the auroral region very slowly, it is difficult to use the relation $x = v_{sat}t$ to infer space derivatives, the velocity of the surge being comparable or larger than the satellite velocity. The applied data treatment has revealed a systematic occurrence of waves at the surge poleward boundary. Shear Alfvén waves ($\Delta B_{tot} \sim 0$ and left-handed polarization) in the period range 180–200 s are likely linked to field line resonance.

Another systematically detected type of waves has a period range of the order of ~30–60 s. These waves are strictly restricted to the most poleward part of the surge and have a zero ΔB also. Recently, *Holter et al*. [1995] interpreted wave observation in a similar frequency range at geosynchronous orbit as confined (standing) ballooning modes trapped in the equatorial current sheet. As the current sheet is disrupted and expands at breakup, the waves could escape and be observed far from the equatorial plane. It must be stressed that the in the wake of dipolarization, *Holter et al*. [1995] observed higher-period (in the 200–500 s range) waves at geostationary orbit. These latter waves were second harmonic standing waves along the entire magnetic field lines, which is strongly reminiscent of the 180–200 s waves reported above and supports the present interpretation that ion injection occurs onto closed field lines.

4.4. Relationship With Midtail Dynamics

Correlations between measurements made onboard Interball and Geotail show that ion injections into the auroral zone are linked to tailward or earthward plasma flows. Although this deserves further studies, it is a strong experimental indication that sporadic ion injections observed at the earthward edge of the plasma sheet are linked to a large-scale plasma sheet instability associated with fast and bursty plasma flows. During a weak substorm, on January 17, 1997 (see Plates 1 and 2 and Figure 2), the plasma sheet instability is found to be located earthward of 30 R_E (Figure 2). During intense substorms the instability which leads to strong earthward plasma flows extends beyond 30 R_E (see Plate 6 and Figure 7). It must be noted that both the cross-tail current disruption model of substorms [e.g. *Lui*, 1996] and the near-Earth neutral line model [e.g., *Shiokawa et al*., 1998] lead to field line dipolarization, directly for the former, and through flow braking for the latter [*Birn et al*., 1996]. The December 22, 1996, case exhibits correlations between injections seen onboard Interball and high flow speed periods seen onboard Geotail. However, these correlations are preliminary and need to be reinforced by dedicated studies.

4.5. Tentative Interpretation of Ion Ejections From the Midtail

Mauk [1986] put forward the idea that the convection surge associated with field line dipolarization can lead to significant parallel ion energization. As a result, bouncing ion clusters and dispersed ion structures may be generated. These transport features however were obtained using guiding center based arguments which are valid only in the innermost magnetosphere (typically, earthward of 10 R_E). In Plate 2, the ions involved in the energy dispersed structures seen after 1240 UT originate from the close tail (~8 R_E) where the model of *Mauk* [1986] can be applied. However, nonbouncing ion dispersed structures (Plates 4, 7, and 8) originate from the relatively distant tail (beyond 15–30 R_E), where the guiding center approximation is violated and where ions behave in a nonadiabatic manner. In this region of space, dispersion signatures more likely result from transitions between distinct nonadiabatic regimes. To illustrate this, consider the particle dynamics in steady state. A parameter, which is widely used to characterize nonadiabatic behaviors, is the parameter κ defined as the square root of the minimum curvature radius to maximum Larmor radius ($\alpha = 90°$) ratio [*Büchner and Zelenyi*, 1989]. For $\kappa > 3$, the motion is adiabatic like in the innermost magnetosphere, whereas for κ of the order of unity or below distinct nonadiabatic regimes can be identified [e.g., *Chen and Palmadesso*, 1986]. In particular, it was shown by *Delcourt et al*. [1996] that pitch angle diffusion near $\kappa = 1$ is organized according to a specific three-branch pattern and can lead to prominent scattering toward small pitch angles (including significant loss cone filling; see also *Sergeev et al*. [1983]. In other words, plasma sheet ions that are subjected to such a scattering will travel down to low altitudes and reach Interball orbit. As κ decreases, the three-branch diffusion pattern successively vanishes and reemerges, thus favoring alternatively trapping or escape from the current sheet as demonstrated by *Delcourt and Martin* [1999]. This can be better appreciated in Figure 9 which shows the magnetic moment scattering (center) and consequent flux variations (bottom) obtained for two distinct κ values. As mentioned above, a well-developed three-branch pattern can be seen for $\kappa = 1.2$ (center right), whereas less clear variations are noticeable for $\kappa = 0.9$ (center left). As a result of this, if one considers an inbound ion population that is isotropic above some limiting pitch angle value (shaded area in the bottom panels), the prominent damping (vertical branch) of magnetic moment at $\kappa = 1.2$ leads to a large outbound flux at small pitch angles (bottom right), whereas for $\kappa = 0.9$, negligible flux is obtained in the parallel direction (bottom left). Behavior as in Figure 9 (left) may in first approximation be expected for κ between ~1 and the first resonance at ~0.5 [e.g., *Chen and Palmadesso*, 1986] whereas that in Figure 9 (right) typically occurs for κ between 1 and 2. This seemingly small (a factor 2) range of κ value actually corresponds to a factor ~16 in energy and the bulk of the ion distribution may thus be affected by this process. As shown by *Chapman* [1994], it is clear from Figure 9 that dynamical reconfigurations of the magnetic field line will lead to similar transitions in plasma sheet ion behaviors. The energy-dispersed structures portrayed in Plates 4, 7, and 8 thus likely follow from modulations of pitch angle in response to relatively small changes in the equatorial magnetic field. The sporadic nature of the injections calls for intermittent changes of the magnetic field line topology and associated electric field.

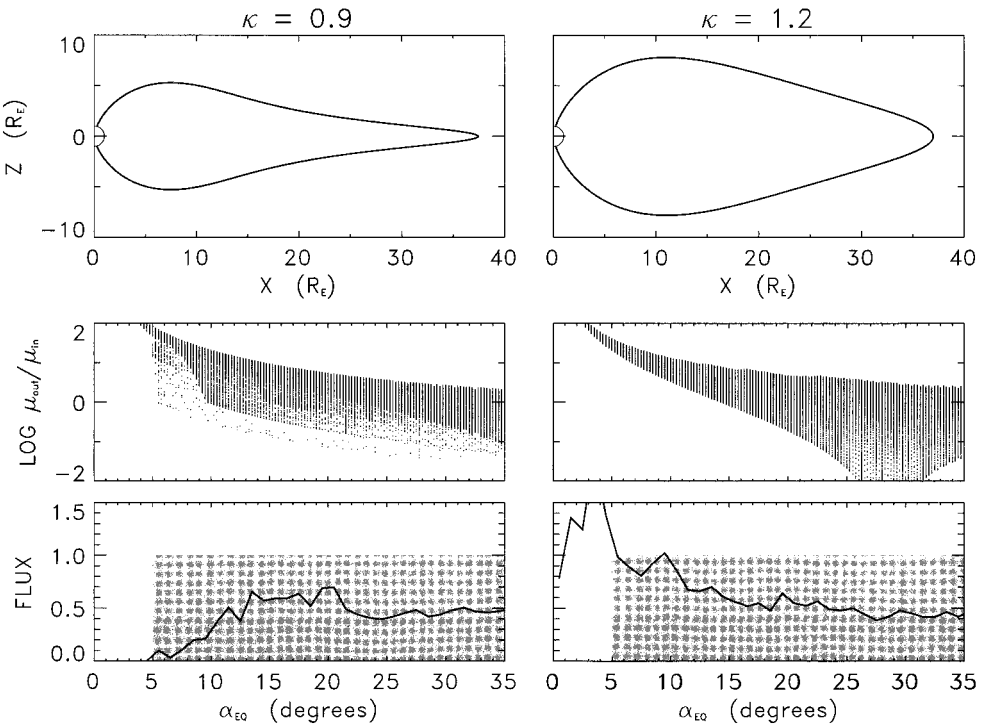

Figure 9. (top) Model magnetic field lines in the midnight meridian plane, (center) magnetic moment (normalized to the initial value) at exit from the current sheet as a function of pitch angle and, (bottom) directional differential particle flux (normalized to unity) as a function of pitch angle. Left and right panels correspond to specific elongations of the magnetic field line, yielding (left) $\kappa = 0.9$ and (right) $\kappa = 1.2$ for 1 keV protons. The pitch angle in the bottom panel is measured at the equator and in the adiabatic limit. Note the loss cone filling for $\kappa = 1.2$.

5. Conclusion

The observational feature of auroral substorm we report in this paper, that is, the recurrent and sporadic injections of magnetospheric ions, is a frequent phenomenon. A statistical analysis of 60 Interball passes at invariant latitudes between 67° and 73° and in the local time sector 21.5–02.5 MLT indicates that time of flight dispersed ion structures (TDIS) are seen in ~35% of the crossings.

Ion dispersions are generally well defined and exhibit a duration at a given energy of the order of 1 min near the poleward border of the bulge. Note that during such a small time period, Interball is nearly stationary. The mechanism responsible for ion ejections from the midtail is thus short lived. The recurrence time of the injections varies from ~1 to 7 mins, and TDIS are detected from the northern border of the auroral bulge down to lower latitudes ($\Delta\lambda > 4°$), indicating they occur on closed field lines. Many cases show well-defined time of flight dispersions extending from the detector upper energy limit (14 keV) down to 1 keV or less. Particle tracing backward in time in 3-D electric and magnetic field models yields a source region near the equatorial plane in the midtail, at distances from ~7 to 40 R_E.

The time of flight dispersions of oxygen ions are at times also observed. Their occurrence is higher during periods of sustained high magnetic activity as is consistent with the enhanced outflow rate from the ionosphere. O^+ trajectory tracing gives results essentially similar to those for H^+. However, it must be stressed that near the bulge poleward front, in several occasions, TDIS display a hard slope with a high-energy cutoff near 3–5 keV. Here we suspect that acceleration/deceleration mechanisms are acting along nonequipotential field lines. Indeed, a modest decelerating parallel electric field, as expected over inverted V regions or perpendicular heating, would reflect particle with low parallel energy before they reach Interball, thus leading to a steepening of the TDIS in the pitch angle range scanned by the ION experiment, i.e., close to 90°. That the bulge poleward boundary is a turbulent region is clearly indicated by the fact that here TDIS are superimposed on a prominent outflow of ionospheric H^+ and O^+. These ions in the hundred of eV to the keV range are mainly heated perpendicularly to the local magnetic field at altitudes close but lower than these of Interball and subsequently transported into the magnetotail. Altogether, these observations provide a new facet of substorm-related acceleration processes.

Acknowledgments. The magnetometer data from the 210MM chain have been kindly provided by K. Yumoyo. The IMAGE magnetometer data used in this paper were collected as a German-Finnish-Norwegian-Polish project conducted by the Technical University of Braunschweig. The LANL geosynchronous data were kindly provided by G. D. Reeves. The authors thank S. I. Klimov and S. A. Romanov for providing Interball-Tail magnetic field data and V. A. Styazhkin for providing Interball-Aurora magnetic field data. This research program has been financed by CNES (contract CNES-08), RKA (contract 035-7534/94), and an INTAS grant (96-2346). Thanks are due to E. Penou (CESR), to Joelle Durand and the data center division from CNES at Toulouse, to Elena Gavrilova and the data center from IKI for reduction and visualization of the ION data.

Janet G. Luhmann thanks Patrick T. Newell and Ingrid Sandahl for their assistance in evaluating this paper.

References

Aggson, T. L., J. P. Heppner, and N. C. Maynard, Observations of large magnetospheric electric fields during the onset phase of a substorm, *J. Geophys. Res*., *88*, 3981, 1983.

Angelopoulos, V., et al., Tailward progression of magnetotail acceleration centers: Relationship to substorm current wedge, *J. Geophys. Res*., *101*, 24,599, 1996.

Bieber, J. W., E. C. Stone, E. W. Hones Jr, D. N. Baker, and S. J. Bame, Plasma behavior during energetic electron streaming events: Further evidence for substorm-associated magnetic reconnection, *Geophys. Res. Lett*., *9*, 664, 1982.

Birn, J., M. Hesse, and K. Schindler, MHD simulations of magnetotail dynamics, *J. Geophys. Res*., *101*, 12939, 1996.

Bösinger, T., and A. G. Yahnin, Pi1B type magnetic pulsation as a high time resolution monitor of substorm development, *Ann. Geophys*., *5*, 231, 1987.

Bosqued, J. M., M. Ashour-Abdalla, M. Elalaoui, V. Peroomian, L. M. Zelenyi, and C. P. Escoubet, Dispersed ion structures at the poleward edge of the auroral oval: Low latitude observations and numerical modeling, *J. Geophys. Res*., *98*, 19,181, 1993.

Büchner, J., and L. M. Zelenyi, Regular and chaotic charged particle motion in magnetotaillike field reversals, 1, Basic theory of trapped motion, *J. Geophys. Res*., *94*, 11,821, 1989.

Chapman, S. C., Properties of single-particle dynamics in a parabolic magnetic reversal with general time dependence, *J. Geophys. Res*., *99*, 5977, 1994.

Chen, J., and P. J. Palmadesso, Chaos and nonlinear dynamics of single-particle orbits in magnetotail-like magnetic field, *J. Geophys. Res*., *91*, 1499, 1986.

Delcourt, D. C., and R. F. Martin Jr., Pitch angle scattering near energy resonances in the geomagnetic tail, *J. Geophys. Res*., *104*, 383, 1999.

Delcourt, D. C., and J. -A. Sauvaud, Plasma sheet ion energization during dipolarization events, *J. Geophys. Res*., *99*, 97, 1994.

Delcourt, D. C., C. R. Chappell, T. E. Moore, and J. H. Waite Jr., A three-dimensional numerical model of ionospheric plasma in the magnetosphere, *J. Geophys. Res*., *94*, 11,893, 1989.

Delcourt, D. C., J. -A. Sauvaud, and A. Pedersen, Dynamics of single-particle orbits during substorms expansion phase, *J. Geophys. Res*., *95*, 20,853, 1990.

Delcourt, D. C., J. -A. Sauvaud, R. F. Martin Jr., and T. E. Moore, On the nonadiabatic precipitation of ions from the near-Earth plasma sheet, *J. Geophys. Res*., *101*, 17,409, 1996.

Delcourt, D. C., J. A. Sauvaud, and T. E. Moore, Phase bunching during substorm dipolarization, *J. Geophys. Res*., *102*, 24,313, 1997.

Delcourt, D. C., N. Dubouloz, J. -A. Sauvaud, and M. Malingre, On the origin of sporadic keV ion injections observed by Interball-Auroral during the expansion phase of substorms, *J. Geophys. Res*., in press, 1999.

Elphinstone, R. D., et al., The double auroral oval distribution, 1, Implication for the mapping of auroral arcs, *J. Geophys. Res*., *100*, 12093, 1995.

Hirahara, M., T. Mukai, T. Nagai, N. Kaya, H. Hayakawa, and H. Fukunishi, Two types of ion energy dispersions observed in the nightside auroral regions during geomagnetically disturbed periods, *J. Geophys. Res*., *101*, 7749, 1996.

Hirahara, M., A. Yamazaki, K. Seki, T. Mukai, E. Sagawa, N. Kaya, and H. Hayakawa, Characteristics of downward flowing ion energy dispersions observed in the low-altitude central plasma sheet by Akebono and DMSP, *J. Geophys. Res*., *102*, 4821, 1997.

Holter, Ø, C. Altman, A. Roux, S. Perraut, A. Pedersen, H. Pécseli, B. Lybekk, J. Trulsen, A. Korth, and G. Kremser, Characteristic of low frequency oscillations at substorm breakup, *J. Geophys. Res*., *100*, 19,109, 1995.

Hones, E. W., Jr., J. R. Asbridge, S. J. Bame, and I. B. Strong, Outward flow of plasma in the magnetotail following magnetic bays, *J. Geophys. Res*., *72*, 5897, 1967.

Hones, E. W., Jr., D. N. Baker, S. J. Bame, W. C. Feldman, J. T. Gosling, D. J. McComas, R. D. Zwickl, J. A. Slavin, E. J. Smith, and B. T. Tsurutani, Structures of the magnetotail at 220 R_E and its response to geomagnetic activity, *Geophys. Res. Lett*., *11*, 5, 1984.

Jacquey, C., J. -A. Sauvaud, and J. Dandouras, Location and propagation of the magnetotail current-disruption during substorm expansion phase: Analysis and similation of an ISEE multi-onset event, *Geophys. Res. Lett*., *18*, 389, 1991.

Jacquey, C., J. -A. Sauvaud, J. Dandouras, and A. Korth, Tailward propagating cross-tail current disruption and dynamics of the near-Earth tail: A multipoint measurement, *Geophys. Res. Lett*., *20*, 983, 1993.

Jacquey, C. D. J. Williams, R. W. McEntire, A. T. Y. Lui, V. Angelopoulos, S. P. Christon, S. Kokubun, T. Yamamoto, G. D. Reeves, and R. D. Belian, Tailward energetic ion streams observed at ~100 R_E by GOTAIL-EPIC associated with geomagnetic activity intensification, *Geophys. Res. Lett*., *21*, 3015, 1994.

Kan, J. R., A globally integrated substorm model: Tail reconnection and magnetosphere-ionosphere response, *J. Geophys. Res*., *103*, 11,787, 1998.

Kokobun, S., T. Yamamoto, M. H. Acuña, K. Hayashi, K. Shiokawa, and H. Kawano, The Geotail magnetic field experiment, *J. Geomagn. Geoelectr*., *46*, 7, 1994.

Kovrazhkin, R. A., J. M. Bosqued, L. M. Zelenyi, and N. V. Jorjio, Reconnection manifestation at 0.5 million km distance in the Earth's magnetic tail (in Russian), *Lett. ZETP*, *45*, 377, 1987.

Lewis, Z. V., S. W. H. Cowley, and D. J. Southwood, Impulsive energization of ions in the near-Earth magnetotail during substorms, *Planet. Space Sci*., *38*, 491, 1990.

Lopez, R. E., and A. T. Y. Lui, A multi-satellite case study of the expansion of a substorm current wedge in the near-Earth magnetotail, *J. Geophys. Res*., *95*, 8009, 1990.

Lui, A. T. Y., A case study of magnetotail current sheet disruption and diversion, *Geophys. Res. Lett*., *15*, 721, 1988.

Lui, A. T. Y., Current disruption in the Earth's magnetosphere: Observations and models, *J. Geophys. Res*., *101*, 13,067, 1996.

Mauk, B. H., Quantitative modeling of the "convection surge" mechanism of ion acceleration, *J. Geophys. Res*., *91*, 13,423, 1986.

Mauk, B. H., and C. E. McIlwain, Correlation of *Kp* with the substorm-injected plasma boundary, *J. Geophys. Res*., *79*, 3193, 1974.

McIlwain, C. E., Substorm injection boundaries, in *Magnetospheric Physics*, edited by B. M. McCormac, p. 143, D. Reidel, Norwell, Mass., 1974.

Mukai, T., S. Machida, Y. Saito, M. Hirahara, T. Terasawa, N. Kaya, T. Obara, M. Ejiri, and A. Nishida, The Low Energy Particle (LEP) Experiment onboard the Geotail satellite, *J. Geomagn. Geoelectr*., *46*, 669, 1994.

Nagai, T., R. Nakamura, T. Mukai, T. Yamamoto, A. Nishida, and S. Kokubun, Substorms, tail flows and plasmoids, *Adv. Space Res*., *20*(4/5), 961, 1997.

Nagai, T., M. Fujimoto, R. Nakamura, Y. Saito, T. Mukai, T. Yamamoto, A. Nishida, S. Kokubun, G. D. Reeves, and R. P. Lepping, Geotail observations of a fast tailward flow at $X_{GSM} = -15$ R_E, *J. Geophys. Res*., *103*, 23,543, 1998.

Nishida, A., T. Mukai, T. Yamamoto, Y. Saito, S. Kokubun, and R. P. Lepping, Traversal of the nightside magnetosphere at 10 to 15 *RE* during northward IMF, *Geophys. Res. Lett*., *24*, 939, 1997.

Ohtani, S, S. Kokubun, and C. T. Russell, Radial expansion of tail current disruption during substorms—A new approach to the substorm onset region, *J. Geophys. Res*., *97*, 3129, 1992.

Pulkkinen, T. I., D. N. Baker, D. G. Mitchell, R. L. McPherron, C. Y. Huang, and L. A. Frank, Thin currents sheets in the magnetotail during substorms: CDAW 6 revisited, *J. Geophys. Res*., *99*, 5793, 1994.

Quinn, J. M., and C. E. McIlwain, Bouncing ion clusters in the Earth's magnetosphere, *J. Geophys. Res*., *84*, 7365, 1979.

Quinn, J. M., and D. J. Southwood, Observations of parallel ion energetization in the equatorial magnetosphere, *J. Geophys. Res*., *87*, 10,536, 1982.

Rostoker, G., J. A. Vallance, R. L. Gattinger, C. D. Anger, and J. S. Murphree, The development of substorm expansive phase—The 'eye'; of the substorm, *Geophys. Res. Lett*., 14, 399, 1987.

Sauvaud, J. -A., and J. R. Winckler, Dynamics of plasma, energetic particles and fields near synchronous orbit in the nighttime sector during magnetospheric substorms, *J. Geophys. Res*., *85*, 2043, 1980.

Sauvaud, J. -A., A. Saint-Marc, J. Dandouras, H. Rème, A. Korth, G. Kremser, and G. K. Parks, A multisatellite study of the plasma sheet dynamics at substorm onset, *Geophys. Res. Lett*., *11*, 500, 1984.

Sauvaud, J. -A., C. Jacquey, T. Beutier, C. Owen, R. P. Lepping, C. T. Russell, and R. J. Belian, Large scale dynamics of the magnetospheric tail induced by substorms: A multisatellite study, *J. Geomagn. Geoelectr*., *48*, 675, 1996.

Sauvaud, J. -A., H. Barthe, C. Aoustin, J. -J. Thocaven, J. Rouzaud, E. Penou, D. Popescu, R. A. Kovrazhkin, and K. G. Afanasiev, The ion experiment onboard the Interball-Aurora satellite; initial results on

velocity dispersed structures in the cleft and inside the auroral oval, *Ann. Geophys*., *16*, 1056, 1998.

Scholer, M, G. Gloecker, B. Klecker, F. M. Ipavich, and D. Hovestadt, Fast moving plasma structures in the distant magnetotail, *J. Geophys. Res*., *89*, 6717, 1984.

Scholer, M. G., D. N. Baker, G. Gloecker, F. M. Ipavitch, A. B. Galvin, B. Klecker, T. Terasawa, and B. T. Tsurutani, Energetic particle-beams in the plasma sheet boundary layer following substorm expansion—Simultaneous nera-earth and distant tail observations, *J. Geophys. Res*., *91*, 4277, 1986.

Sergeev, V. A., and A. G. Yahnin, The features of auroral bulge expansion, *Planet. Space Sci*., *27*, 1429, 1979.

Sergeev, V. A., E. M. Sazhina, N. A. Tsyganenko, J. A. Lundblad, and F. Soraas, Pitch-angle scattering of energetic protons in the magnetotail current sheet as the dominant source of their isotropic precipitation into the nightside ionosphere, *Planet. Space Sci*., *31*, 1147, 1983.

Sergeev, V., R. C. Elphic, F. S. Mozer, A. Saint-Marc, and J. -A. Sauvaud, A two-satellite study of nightside flux transfer events in the plasma sheet, *Planet. Space Sci*., *40*, 1551, 1992.

Sergeev V., T. I. Pulkkinen, and R. J. Pellinen, Coupled-mode scenario for the magnetospheric dynamics, *J. Geophys. Res*., *101*, 13,047, 1996.

Sergeev, V., et al., Plasma sheet ion injections into the auroral bulge: Correlative study of spacecraft and ground observations, *J. Geophys. Res.*, in press, 1999.

Shiokawa, K., W. Baumjohann, G. Haerendel, G. Paschmann, J. F. Fennell, E. Friss-Christensen, H. Luhr, G. D. Reeves, C. T. Russell, P. R. Sutcliffe, and K. Takahashi, High speed flow, substorm current wedge, and multiple Pi 2 pulsations, *J. Geophys. Res*., *103*, 4491, 1998.

Tighe, W. G., and G. Rostoker, Characteristics of westward travelling surges during magnetospheric substorms, *J. Geophys. Res*., *50*, 51, 1981.

Torr, M. R., et al., A far ultraviolet imager for the international solar-terrestrial physics mission, *Space Sci. Rev*., *71*, 329, 1995.

Tsyganenko, N. A., A magnetospheric magnetic field model with a warped current sheet, *Planet. Space Sci*., *37*, 5, 1989.

Volland, H., A model of the magnetospheric convection electric field, *J. Geophys. Res*., *83*, 2695, 1978.

Weimer, D. R., A flexible, IMF dependent model of high latitude electric potentials having "space weather" applications, *Geophys. Res. Lett*., *23*, 2549, 1996.

Winckler, J. R., The origin and distribution of energetic electrons in the Van Allen radiation belts, in *Particles and Fields in the Magnetosphere*, edited by B. M. McCormac, p. 332, D. Reidel, Norwell, Mass., 1969.

Yahnin, A. G., T. Bösinger, J. Kangas, and R. D. Belian, Some implications on substorm dynamics inferred from correlations between multiple flux peaks of drifting protons clouds and ground observations, *Ann. Geophys*., *8*, 327, 1990.

M. Brittnacher and G. K. Parks, Geophysics Department, University of Washington, Seattle, WA 98195.

D. C. Delcourt, Centre d'Etude des Environnement Terrestres et Planétaires, Saint-Maur des Fossés, France.

S. Kokubun, Solar Terrestrial Environment Laboratory, Nagoya University, 386-1298 Shimonogo 658-1, Ueda City, Nagano, Japan.

R. A. Kovrazhkin, Institute of Space Research, 117810, Moscow GSP-7, Profsoyuznaya, 84/32, Russia.

T. Mukai, Institute of Space and Astronautical Science, 3-1-1 Yoshinodai, Sagamihara, Kanagawa 229-8510, Japan.

D. Popescu and J. -A. Sauvaud, Centre d'Etude Spatiale des Rayonnements, 9 Avenue du Colonel Roche, BP 4346, 31028 Toulouse, France.

V. Sergeev, University of St. Petersburg, Universitetskaya emb., 7/9, St. Petersburg, 199034, Russia.

(Received March 25, 1999; revised June 28, 1999;
accepted June 28, 1999.)